Heat stress induces unreduced male gamete formation by targeting the meiotic cyclin TAM/CYCA1;2

Authors: Cédric Schindfessel[1], Chunlian Jin[1#], Danny Geelen[1*]

[1] Department of Plants and Crops, unit HortiCell, Faculty of Bioscience Engineering, Ghent University, Coupure Links 653, 9000 Ghent, Belgium.

[#] Current affiliation: National Engineering Research Center for Ornamental Horticulture, Key Laboratory for Flower Breeding of Yunnan Province, Floriculture Research Institute, Yunnan Academy of Agricultural Science, Kunming, China.

*corresponding authors: danny.geelen@ugent.be

ABSTRACT

Heat stress promotes the formation of unreduced (2n) male gametes, a driving force of evolutionary polyploidization in the plant kingdom. Here we report that the molecular mechanism underlying heat tolerance of the reproductive system in Arabidopsis thaliana relies on sustained synthesis of the cell cycle protein TAM/CYCA1;2. Under heat stress TAM protein accumulates in stress granules when expressed from a gene that is derived from a heat tolerant Arabidopsis accession such as Col-0. Heat sensitive TAM alleles do not support TAM protein synthesis at elevated temperatures resulting in over 80% of the pollen being diploid. However, sustained expression of TAM is not sufficient as heat stress also promotes formation of unreduced male gametes in Col-0 mutants of the meiosis exit regulators THREE DIVISION MUTANT1 (TDM1) and SUPPRESSOR WITH MORPHOGENETIC EFFECTS ON GENITALIA7 (SMG7). These findings reveal a TDM1 and SMG7 dependent licencing mechanism securing protein synthesis and male meiosis progression under heat stress conditions. Arabidopsis accessions that do not possess this heat tolerant translation mechanism are poised to produce high frequencies of unreduced male gametes and generate polyploid offspring at elevated temperature.

Keywords: meiosis, temperature, restitution, progression, translation, polyploidisation, evolution

INTRODUCTION

Plant genomes feature the remnants of past whole genome duplications that contribute to gene and species evolution [1]. These events of autopolyploidization have arisen either from somatic chromosome doubling or sexually through the fusion of unreduced gametes[2]. Sexual polyploidization has been reported for a wide variety of plant species and is considered the main route to polyploidy [3,4] . The reproductive system happens to be also the most temperatures sensitive developmental phase of a plant due the complexity of the molecular processes underlying flowering, development of the reproductive organs, gametogenesis, fertilization, and seed development [5]. While in general heat stress reduces fertility by inducing cell death, the impact on the ploidy of microspores and pollen arises from a defect in meiosis whereby either the first or second meiotic division is omitted, a phenomenon known as meiotic restitution [6,7]. High temperature conditions during meiosis promote meiotic restitution and (unreduced) diploid pollen formation (2n) [8]raising the incidence of polyploidization events.

In the light of global increase in temperature it is of interest to determine what genetic factors determine meiotic restitution. Unreduced male gametes are formed by mutants defective in the cell cycle progression regulators TARDY ASYNCHRONOUS MEIOSIS (TAM/CYCA1;2) [9,10], OMISSION OF SECOND DIVISION1 (OSD1) [11], and multiple CYCLIN DEPENDENT KINASES (CDKs) [12,13]. Mutations in these genes deregulate the meiotic progression pathway, that also involves the ANAPHASE PROMOTING COMPLEX/CYCLOSOME (APC/C), leading to the formation of dyad microspores. The termination of meiosis on the other hand requires the evolutionarily conserved nonsense-mediated RNA decay (NMD) factor SUPPRESSOR WITH MORPHOGENETIC EFFECTS ON GENITALIA7 (SMG7) and the plant specific protein THREE-DIVISION MUTANT1 (TDM1) [14–17]. In meiocytes, TDM1 and SMG7 are loaded into P-bodies and stimulate meiotic exit through sequestration of the translation initiation complex elF4F [17]. Remarkably, the inability of the *tdm1-3* mutant to exit meiosis is rescued by cycloheximide providing evidence for a central role of translation inhibition in terminating meiosis [17]. Premature exit of meiosis after the first division is prevented by phosphorylation of TDM1 by CDKA;1-TAM [18].

Alternatively, meiotic restitution results from defects in chromosome segregation as observed in mutants of *JASON*, *PARALLEL SPINDLE1* (*PS1*), *DUET/MALE MEIOCYTE DEATH1*

(*MMD1*) and *FORMIN14* (*AFH14*) that regulate, separately or in combination, the organisation and orientation of the meiotic spindles [19–23]. In these mutants, meiosis I proceeds into meiosis II and during the second meiotic division parallel or fused spindles form, re-joining the sister chromatids from the homologous chromosome pairs.

Although heat-induced meiotic restitution has been extensively reported in a variety of plant species [8,24–28], the mechanism by which high temperature alters meiosis remains elusive. Here, we identified allelic variations of TAM/CYCA1;2 responsible for the heat-sensitive meiotic restitution in natural, *Arabidopsis* accessions. In addition, we show that heat stress induces premature meiotic exit in *tdm1-3* and *smg7-6*, inhibitors of protein translation and regulation of meiosis exit. These results reveal that natural variation in heat sensitive meiotic restitution in Arabidopsis populations is due to the differential capacity of sustaining protein synthesis under conditions of heat stress. Our results provide a molecular link between periods of high temperature conditions and evolutionary events of plant polyploidization.

RESULTS

Natural variation in heat induced meiotic restitution in Arabidopsis

We exposed 212 natural *Arabidopsis thaliana* accessions from different climatological regions to 32°C for 24h and compared their tetrad-stage of male meiosis to a 20°C control. The formation of tetrads, triads and dyads (Figure 1a, b, c) was recorded to determine the incidence of defects in male meiosis under high temperature stress. Across these accessions grown under control conditions (20°C), a total of 2 dyads and 1 triad were recorded among 44405 tetrad-stage configurations viewed. All other microspores appeared as tetrads, showing that male meiosis robustly results in 4 haploid microspores at the end of meiosis in a wide variety of *Arabidopsis thaliana* accessions. After heat treatment a total of 8174 dyads, 1411 triads and otherwise tetrads were recorded out of 84975 microspores, indicating that meiotic restitution as a response to changing environmental temperature is a widespread phenomenon in Arabidopsis. Remarkably, the dyad production after heat varied largely between accessions, with average dyad production ranging from 0% to nearly 100% (Figure 1d), indicating that intra-species genetic variation is responsible for the variation in meiotic restitution rates.

Correlating the dyad frequency of all accessions with 64 climatological variables of the CHELSEA Bioclim high resolution data set [29] revealed no significant correlations (Supp. Table 1) and the high dyad producing accessions could not be clearly separated from the others based on a principal component analysis using the same climatological variables (Supp. Figure 1). These data suggest that there is no direct link between high rates of heat induced meiotic restitution and the accessions' geographical or climatological origin.

Next, we used our most heat sensitive lines to test the hypothesis that unreduced gametes evoked by a stressful environment can lead to plant polyploidisation events [30–32]. Since pollen size is known to increase with increasing ploidy levels [33], we monitored the downstream pollen development of heat induced dyads and observed the production of enlarged pollen grains in multiple high dyad producing lines (Figure 1e-h; Supp. Note 1). Furthermore, we confirmed that these enlarged pollen grains are viable, unreduced gametes by using them in manual crosses to induce triploid (3n) offspring (Figure 1i-j; Supp. Note 1).

Heat sensitive TAM alleles lead to meiotic restitution

We mapped the locus responsible for the high dyad phenotype of accession Mt-0 to *TAM/CYCA1;2* (see Methods), a well-studied meiotic cyclin [9,10,16,18]. Mutants of *tam* skip the second meiotic division and produce dyads and unreduced pollen under standard growth conditions. The TAM defect in Mt-0 at high temperatures was confirmed by allelism test crosses with 2 independent mutant alleles in the F1 (Figure 2a). Histological examination showed that Mt-0 dyads are formed because of an arrest of the second meiotic division at high temperature, but that the defect originates from a heat sensitivity in meiosis I (Supp. Note 2). This is in line with the known molecular function of TAM acting on meiosis I to II progression [16,18].

Subsequently Mt-0 and L*er* were used as tester lines to complement heat sensitive accessions revealed in our initial tetrad-stage screen. Several F1 lines were generated, and tetrad-stage microspores were analysed after a 24h at 32°C treatment. For 7 accessions it was found that they were unable to complement the heat induced dyad phenotype of Mt-0, whereas in crosses with Ler, the dyad phenotype was suppressed (Figure 2b). These results validate *TAM* as the heat sensitive gene leading to dyad formation in at least 8 natural accessions of *Arabidopsis thaliana*.

High temperature interferes with TAM expression

Next we analysed the TAM protein using C-terminally GFP-tagged constructs of the Col-0 and Mt-0 allele (respectively a low and high dyad producing accession after heat) in the tam-1 background. Under control conditions (20°C), the TAM-GFP expression peaks during mid to late prophase (Figure 3). Around zygotene, the TAM-GFP signal congregated into distinct cytosolic foci (Figure 3a). At 32°C the lines carrying the Col-0 *TAM* allele showed no remarkable difference in foci formation and foci number compared to 20°C (Figure 4a, b and Supp. Figure 2). On the contrary, in the lines with the Mt-0 *TAM* allele, high temperature conditions significantly decreased the expression and the number of foci (Figure 4a, b and Supp. Figure 2), showing that reduced TAM protein levels correlate with the high frequency of dyad production.

Because heat sensitive lines might carry a conditional knock-out allele of TAM, we compared the relative TAM expression levels in flower buds of plants grown at 20°C and after 24h 32°C (Figure 4c). qPCR analysis showed that *TAM* expression levels slightly increased upon heat treatment in both heat sensitive (Mt-0, Vimmerby, Nok-3, Etna-2, Tac-0, tam-1) and heat tolerant accessions (Col-0, Zdr-1).

To eliminate the effect of the different genetic backgrounds we also compared the TAM expression in the heterozygous F1 Mt-0/tam-2, Col-0/tam-2 and Mt-0/Col-0 at 20°C and 32°C (Figure 4d). Although the TAM expression in Mt-0/tam-2 and Col-0/tam-2 is about half compared to Mt-0/Col-0, all 3 lines produced 100% normal tetrads at 20°C (Figure 2a). After 24h at 32°C, *TAM* expression levels in all 3 lines were not significantly changed compared to their respective 20°C control (Figure 4d), but the Mt-0/tam-2 produced nearly 100% dyads, whereas Mt-0/Col-0 and Col-0/tam-2 produced mainly tetrads (Figure 2a). This indicates that changes in *TAM* transcription rates cannot explain the high dyad phenotype in Mt-0.

As TAM is a target of the APC/C and degradation by the 26S proteasome [15] we then hypothesised that the reduced Mt-0 TAM expression was caused by premature degradation of the protein. This was tested by blocking protein degradation with the proteasome inhibitor MG132. Treatment with MG132 slightly increased the number of TAM foci in the lines expressing the Col-0 or the Mt-0 construct (Figure 4e and Supp. Figure 3), and produced monads, dyads and triads next to tetrads at 20°C (Supp. Figure 4), in line with the known

requirement of protein degradation to ensure proper meiotic progression [15,34]. MG132 treatment in combination with 24h at 32°C resulted in an increase of Col-0 TAM-GFP foci whereas Mt-0 TAM-GFP expression dropped below detection (Figure 4e and Supp. Figure 3). These results indicate that the 26S proteasome is not causing the decrease in Mt-0 TAM protein at 32°C.

We then suspected that Mt-0 TAM protein synthesis is somehow affected by the heat stress treatment. To counter the effect of high temperature treatment on protein synthesis, we applied complementary peptides (cPEPs) that selectively increase the translation of a specific protein [35]. Two synthetic cPEPs that putatively boost TAM protein synthesis were applied to heat treated Mt-0 flower buds. Treatment with the cPEPs significantly decreased the dyad production frequency in heat treated Mt-0 by about 20% compared to the mock (Figure 4f). Boosting Mt-0 TAM protein synthesis therefore partially rescued the temperature sensitivity, suggesting that heat stress prevents regular TAM expression by inhibiting protein translation.

High temperature inhibits meiotic protein translation

It was recently shown that meiotic exit in Arabidopsis is activated by TDM1 and SMG7 through sequestering of the protein translation complex eIF4F complex to P-bodies [17]. Mutants of *tdm1* or *smg7* are unable to inactivate the eIF4F protein translation machinery, resulting in continued cell divisions without DNA replications and formation of hypoploid spores with irregularly organized callose walls (Figure 5a-c). Dependence of meiotic exit on TDM1 is overruled by cycloheximide treatment blocking translation and forcing meiotic exit [17]. Heat stress has a similar impact as cycloheximide as *tdm1-3* and *smg7-6* mutants exposed for 24h at 32°C show meiotic exit and produce dyads, triads and tetrads instead of hypoploid spores (Figure 5d-g). The frequency of dyad formation in the *tdm1-3* background was about 20% higher compared to the *smg7-6* mutant and independent of the TAM allele (Col-0, Mt-0, *tam-2*) (Figure 5g). These findings suggest that TDM1 has a more prominent role in controlling the activity of the eIF4F protein translation machinery at the end of meiosis I.

DISCUSSION

Sexual reproduction is sensitive to high temperatures, with heat stress during gamete development often leading to temporal sterility and meiotic defects. Meiotic restitution and

the production of unreduced gametes is a common defect observed in plants under heat stress[8,24–26,28]. It has been suggested that an instable climate could induce the formation of these 2n gametes, leading to plant polyploidization events and the creation of genetic diversity [31]. Uncovering a molecular framework for heat-induced meiotic restitution would greatly help to establish such a link more firmly.

In this work, we present the identification of allelic variations of the core meiotic cyclin TAM/CYCA1;2 responsible for heat induced dyad formation in high temperature hypersensitive *Arabidopsis* accessions. As TAM null mutants produce only dyads, we assume that heat stress inactivates TAM in the hypersensitive lines while heat tolerant lines maintain TAM expression and activity. TAM mRNA levels are not changed by heat, instead, the TAM protein and the cytoplasmic foci to which TAM is sequestered, are strongly reduced under heat stress. By boosting TAM translation using cPEPs [35] regular microspore formation is improved whereas blocking the proteasome does not alleviate the dyad phenotype. These results point out that TAM translation is a primary target of heat stress.

Translation is dynamic and regulates progression of meiosis in yeast and mammals [36–38]. In plants, meiotic exit is specifically under TDM1 and SMG7 control of translation [17]. TDM1 is suppressed by CDKA;1-TAM phosphorylation at the end of meiosis I, presumably to prevent its interaction with translation elongation factors such as elF4isoG2 (Figure 6). At the end of meiosis II, TDM1 as well as the elF4G/F translation initiation complex is recruited to P-bodies by SMG7, and hence no longer allows translation to take place which has been shown to promote exit of meiosis using cycloheximide [17]. Under heat stress conditions, TAM and CDKA;1 associate with stress granules (SGs) and no longer can phosphorylate TDM1 (Figure 6). Depending on the capacity of the Arabidopsis accession to continue to produce TAM protein, a smaller or larger number of the meiocytes will execute premature meiosis exit. The model in Figure 6 also illustrates how heat stress applied to tdm1-3 and smg7-6 mutants causes premature exit while these proteins paradoxically activate meiosis exit. Under heat stress conditions, the P-bodies may converge or associate with stress granules, thereby sequestering the protein translation machinery from its free form, such that translation is no longer active and the inhibition of meiosis exit relieved (Figure 6). TAM and CDKA;1 are also sequestered into SGs which might be necessary for SG dissolution and continuation of the cell cycle after stress relief [39].

TAM is not likely the only protein affected by heat as high temperature stress causes a general inhibition of translation [40–43]. Heat stress triggered translational shut-down is accompanied by the preferential licensing of translation of specific stress-protection HEAT SHOCK FACTORS (HSF) and heat induced chaperones, which are required to restore the heat inflicted damage [43]. HEAT SHOCK PROTEIN (HSP101) of maize, for instance, ensures double strand break repair, cross over fidelity, and fertility at high temperature conditions by releasing ribosomal protein mRNAs from ribonucleoprotein granules, allowing protein translation [43–45]. Also, the cell cycle arrests under high temperature conditions which is associated with the sequestration of cell cycle proteins into SGs [46,47]. These findings strongly suggest that heat tolerant Arabidopsis lines have evolved to develop a mechanism that mitigates heat stress induced meiotic cell cycle arrest by licensing the translation of key regulators like TAM. That mainly TAM allelic variants were found in our screen, points to the importance of rebooting the cell cycle when temperature drops back to favourable conditions, with TAM as a key regulator.

The impact of heat stress on gametogenesis is very diverse and depends on the heat stress conditions and the species [5,30]. Several studies reporting alterations in meiotic recombination, synapsis, and chromosome dynamics fail to link these defects with the depletion of meiotic proteins [48]. In view of the general inhibition of protein translation upon heat stress, licencing protein translation might play a prominent role in multiple aspects of meiosis under high temperature and the genetic variation in specific genes may generate the diverse phenotypes observed across species. Our data also implies that attempts to regulate the translatome of developing gametes, for example through the use of complementary peptides [35], could secure crop fertility under elevated temperature conditions.

MATERIAL AND METHODS

Plant material and growth conditions

For the initial tetrad-stage screen, 212 natural Arabidopsis accessions were selected [49]. The tam-1 seeds were kindly provided by Ming Yang (Oklahoma State University) and Raphael Mercier (Max Planck Institute for Plant Breeding Research) provided the tam-2 and tdm1-3 lines. Genotyping primers are shown in Supp. Table 4.

Seeds were sterilized using chlorine gas and sown on growth medium (for 1l of medium: 2.154g MS without vitamins, 10g sucrose, 100mg myo-inositol and 0.5g MES, 8g agar. pH adjusted to 5.7. 50mg kanamycin was added for antibiotic selection). Seeds were vernalised for 3 days at 4°C in the dark and moved to 21°C and 16h/8h light/dark for germination. After 5 days, seedlings were transferred to soil substrate (Jiffy) and grown at 20°C under 12h/12h light/dark for 3-4 weeks with regular watering supplemented with liquid fertilizer (Wuxal). Afterwards, plants were grown at 20°C and 16h/8h light/dark without fertilizer to stimulate flowering. Relative humidity was kept at 60%-70%. For experiments after the initial tetrad-stage screen, a 10 week cold treatment at 4°C and 16h/8h light/dark was used for accessions Vimmerby, Nok-3, Tac-0, Ta-0, Etna-2, TOM03, Sorbo, Or-1, Tha-1, before moving them to 20°C to stimulate even flowering.

For temperature experiments, healthy looking, flowering plants with at least 3 siliques on the main inflorescence axis were transferred to a Panasonic MLR-352H-PE versatile environmental test chamber under similar growing conditions, but with different temperatures (4°C, 28°C, 32°C) for the duration of the treatment (12h, 24h, 48h).

Tetrad-stage analysis

Accessions were divided into 54 batches (G1-G54) based on their flowering time under 16h/8h light/dark. Three plants for every accession were kept at 20°C and 10 plants were heat treated for 24h at 32°C. Immediately after the treatment, tetrad-stage flowerbuds of the main inflorescence were dissected and stained with lactopropionic orcein [8]. For every individual plant the number of tetrad-, triad- and dyad-configurations was recorded. Accessions with at least 3 individual heat treated plants with at least 20 tetrad-stage configuration counts were selected for further analysis (a total of 172 accessions; Supp. File 1). The number of tetrads, triads and dyads were converted to a percentage for every plant and the mean value and standard error were calculated for every accession and treatment. A Kruskal-Wallis rank-sum test on the mean dyad production revealed no batch effect ($p=0.32$).

Aniline blue staining of tetrad-stage microspores to stain the callose walls was done according to [50].

Climate variables analysis

The data on 64 climate variables for the earth's surface from the CHELSEA Bioclim dataset [29] were downloaded from https://chelsa-climate.org/. For every Arabidopsis accession with a known geographical location (longitude, latitude) the values on these climate variables for their respective location were extracted from the dataset and used for correlation analysis with the dyad production frequency after 24h at 32°C and principle component analysis using custom R scripts.

Male meiotic chromosome spreads

DAPI staining of enzyme digested chromosome spreads of male meiotic flowerbuds was done according to [51] with modifications mentioned in [8]. The same technique was used to observe somatic chromosome spreads.

F2 mapping analysis

The F2 generation of a cross between Ler and Mt-0 was heat treated (24h 32°C) during the flowering stage and individual plants were checked for high dyad production at the tetrad-stage. The outcross analysis revealed that the dyad phenotype of Mt-0 is linked to a single recessive locus (Supp. Table 5). Leaf samples of the high dyad producing plants were stored at -80°C before DNA extraction with the Wizard genomic DNA purification kit (Promega). A pooled DNA sample (equal mass) was sent for sequencing on an Illumina NextSeq500 PE150 platform for a total of 36Gb output (predicted coverage: 60x). Adapter and low quality reads were removed with Trimmomatic v0.39 using standard parameters [52]. Duplicate reads were removed with FastUniq v1.1 [53] and quality was monitored using FastQC v0.11.2 [54]. Aligning, mapping and annotation were performed with SHOREmap v3.0, according to [55]. This mapped the responsible locus to a 2.4Mbp region on the bottom of chromosome 1 (Supp. Figure 5), which contains TAM.

Analysis of SNP frequencies

SNP and indel frequencies for the genomic positions of the TAM locus (chr1: 29081654..29085477) were extracted from the 1001 genomes database (https://tools.1001genomes.org/polymorph/) [56], or our own resequencing data in case of Mt-0.

Positions of relevant genomic regions and functional protein domains were extracted from EnsemblPlants (https://plants.ensembl.org/index.html). Data were reformatted using custom made R scripts.

Two-step RT-qPCR

Immediately after the treatment (20°C or 24h at 32°C) all unopened flowerbuds on the main axis were frozen in liquid N_2 before RNA extraction using the Promega ReliaPrep RNA Tissue Miniprep System. RNA purity and quantity were checked with Nanodrop and 1µg of total RNA was used as starting material for first strand cDNA synthesis using the Promega GoScript Reverse Transcription System with oligo(dT) primers. Two µl of cDNA (1:4 dilution) was added to a 20µl qPCR reaction using the GoTaq qPCR Master Mix (Promega) and ran on a BioRad CFX Opus96 thermocycler. Cycles were as follows: 2min at 95°C, 40x (15s at 95°C and 40s at 60°C). Quality was checked by melting curve analysis and gel electrophoresis of the PCR products. For each accession 3 individual plants were used per treatment (biological replicates) and 3 technical replicates were performed per sample. Data were analysed using the ΔΔCt method as described in [57] using the R pcr package [58], with EF1αA4 as the reference gene [48], and normalized to the 20°C control for each accession. Primers are shown in Supp. Table 4.

Plasmid construction and transformation

Gene cloning was performed with the Multisite-Gateway cloning system (Invitrogen). Primers for cloning the TAM upstream and RNA genomic regions are given in Supp. Table 4. Plasmids were checked through enzyme digestion and sequencing before moving them to Agrobacterium tumefaciens strain GV3130. Floral dip was used to transform tam-1 plants. Transformed plants were selected based on kanamycin resistance and complementation of the tam-1 phenotype at 20°C.

Pollen particle size analysis

A single, freshly opened flower was picked from the main inflorescence and placed in 1ml of Isoton II solution. After vortexing to release the pollen and removal of the flower material the solution was diluted in 10ml of Isoton II and measured using a Beckman Mulitisizer II

Coulter counter as previously described [33]. For each treatment 3 or 4 individual plants were used that produced 1-3 open flowers on the main inflorescence per day. Analysis based on size thresholds was done using a custom R script. Samples with less than 200 particle counts were removed from the particle size analysis.

Alexander staining of mature pollen

After dissecting the anthers from nearly opened flowers (before anther dehiscence), viability staining was performed as described by Alexander (1969).

DAPI staining of mature pollen

To visualise the nuclei in mature pollen grains, open flowers were placed in 200µl of citrate-phosphate buffer at pH 4, with 1% triton X-100 and 1µg/ml DAPI [60]. After vortexing and removal of the flower material samples were incubated for 20min in the dark. The solution was centrifuged to pellet the pollen and the pellet was resuspended in 20µl of staining solution before visualisation.

Plant ploidy analysis

Somatic ploidy determination was done based on the nuclear extraction method described by Galbraith et al. (1983) on fresh leaf material as described by De Storme & Geelen (2011). Propidium iodide stained samples were analysed on a BD FACSVerse flow cytometer.

DAPI and SR2200 staining of intact anthers

DAPI and SR2200 staining of male meiocytes in intact anthers was performed as described by Capitao et al. (2021). For consistency and to avoid fading of any GFP signal, samples were fixed and prepared for visualisation under a microscope within a single day.

MG132 and peptide treatment of in vitro grown inflorescences

For in vitro cultivation of Arabidopsis inflorescences the protocol of Prusicki et al. (2019) was adapted. After removing the largest flowerbuds, the stem of an inflorescence was cut

with a clean razor blade about 0.5cm under the flowerbuds. The inflorescence was positioned in the middle of a well in a 24-well plate filled with 1ml of Apex Culture Medium (ACM; 2.2g/L MS medium, 10 g/L sucrose, 8 g/L agarose, pH 5.8) with vitamins (1000x stock: 10% myo-inositol, 0.1% nicotinic acid, 0.1% pyridoxin hydrochloride, 1% thiamine hydrochloride, 0.2% glycine). The plate was closed and the inflorescences were left to climatise in a growth chamber at 20°C in the light for 4h. Afterwards a volume of 500µL liquid ACM (without agarose) supplemented with 100µM MG132 or an equal volume of DMSO was placed on top of the inflorescences, submerging them completely. Subsequently the plate was moved to a climate chamber set at 20°C or 32°C for a 24h treatment followed by immediate fixation of the samples before analysis.

For the peptide treatments, 100µM of a peptide or an equal volume of water was dissolved in the ACM medium with agarose at the bottom of each well. Cut inflorescences were transplanted in the medium and submerged in 500µL liquid ACM medium supplemented with 100µM peptide or an equal volume of water for 24h at 20°C. The liquid was then removed before a heat treatment of 24h at 32°C, followed by immediate fixation of the samples before analysis. Peptide sequences are given in Supp. Table 4.

Microscopy

Microscopic images were taken using an Olympus IX81 microscope with an X-Cite 120 LED boost lamp equipped with an Olympus XM10 camera and Olympus Cell M software. Images after Alexander staining were taken on an Olympus BX51 with a ColorView III camera and Cell F software. For confocal microscopy, images were taken on a Nikon A1R HD25 and analysed with Nikon NIS-elements software.

Statistical analyses

Statistical analyses and methods are detailed in the relevant figure or table captions and the relevant text sections.

ACKNOWLEDGMENTS

The authors would like to thank Ming Yang for providing the tam-1 seeds and Raphael Mercier for the tam-2 and tdm1-3 seeds. We thank Albert Cairo and Karel Riha for providing the protocol for staining of intact Arabidopsis anthers. Limin Sun and Robin Lardon are thanked for the helpful discussions. We thank Steffen Vanneste for critical reading of the manuscript. We are grateful to Christophe Petit, Ellen Van Gysegem and Patricia Delaere for technical support. This work was supported by the Research Foundation-Flanders (FWO), through a Ph.D. fellowship to Cédric Schindfessel (Grant No. 11G7421N) and Chunlian Jin was supported by CSC grant No. 201606350011.

AUTHOR CONTRIBUTIONS

CS and DG designed the experiments. CS and CJ performed the experiments. CS analysed and visualised the data. CS and DG wrote the manuscript.

COMPETING INTERESTS

The authors declare no competing interests

FIGURES AND TABLES

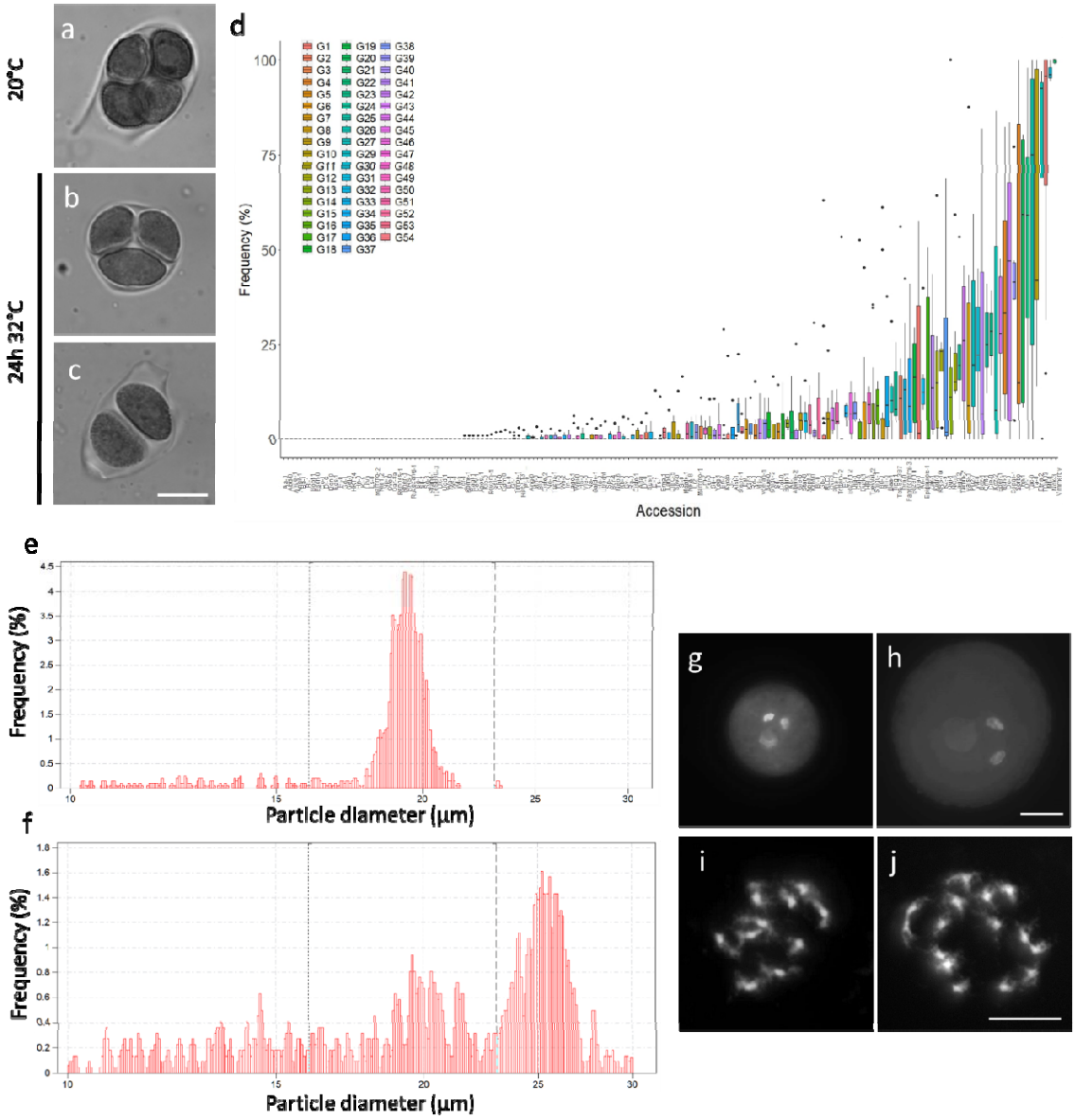

Figure 1 Natural variation in heat induced meiotic restitution in Arabidopsis.

a-c) Orcein stained tetrad-stage male meiocytes. Example of a tetrad under 20°C control conditions **(a)** and a triad **(b)** and a dyad **(c)** after a 24h at 32°C heat treatment. Scale bar = 10µm. **d)** Frequency of dyad production after 24h at 32°C for all 172 accessions analysed, ranked according to average dyad frequency. Boxes are coloured according to the batch the accession was analysed in (G1-G54). Lower and upper hinges of the box correspond to the first and third quartile. Whiskers extend from the hinges no further than 1.5 times the inter-quartile range (or to the highest or lowest data point). Data points beyond the range of the whiskers are plotted separately. **e-f)** representative example of the pollen particle size distribution of Mt-0 plants kept at control conditions (20°C; **e**) and plants heat treated for 24h at 32°C **(f)**. The vertical dotted and dashed lines mark the particle sizes of 16µm and 23µm respectively. **g-h)** DAPI stained images of control (20°C) pollen **(g)** and enlarged pollen of Mt-0 after heat treatment **(h)**. Scale bar = 10µm. **i-j)** DAPI stained, enzyme digested mitotic chromosome spreads of a diploid (2n=10; **i**) and a triploid (3n=15; **j**) Mt-0 plant after heat treatment and self-fertilization. Scale bar = 10µm.

a

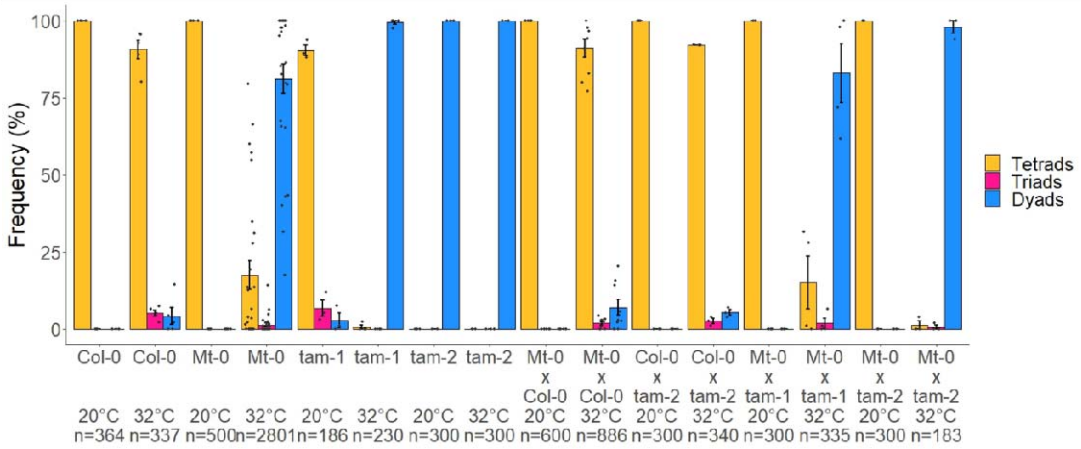

b

Female \ Male	**Mt-0**	**Vimmerby**	**Ta-0**	**Tac-0**	**Etna-2**	**Or-1**	**Nok-3**	**Tha-1**	**Ler**
Mt-0	81+-25	76+-47	73+-17	96+-7	61+-?	69+-29	98+-6	50+-3	3+-3
Vimmerby	-	100+-1	-	-	-	-	-	-	-
Ta-0	-	93+-6	51+-42	62+-35	-	-	-	-	-
Tac-0	-	91+-14	-	54+-34	-	-	-	-	-
Etna-2	-	97+-5	-	-	58+-38	-	-	-	-
Or-1	-	-	-	-	-	45+-34	-	-	-
Nok-3	-	-	-	-	-	-	77+-32	-	-
Tha-1	-	-	-	-	-	-	-	43+-43	-
Ler	-	9+-6	4+-4	6+-10	1+-1	1+-1	1+-2	5+-3	1+-1

Figure 2 Heat sensitive TAM alleles are responsible for meiotic restitution in at least 8 Arabidopsis accessions.

a) Frequency (%) of the different configurations (tetrads, triads or dyads) observed at the tetrad-stage of various lines and their heterozygous F1 under control conditions (20°C) and after a 24h at 32°C heat treatment. n represents the number of individual meiocytes counted. Error bars represent standard errors. A minimum of 3 plants were analysed for every treatment, represented by black dots. **b)** Dyad frequency at the tetrad-stage after 24h at 32°C for different F1 hybrids between several high dyad producing accessions and the Mt-0 and Ler tester lines. The diagonal represents the values for the individual natural accessions. Values are presented as the average dyad frequency +- standard deviation. Data were collected from at least 3 individual F1 plants per cross, except for the cross Mt-0xEtna-2 from which only 1 plant was available. Source data and sample sizes in Supp. File 1 and Supp. Table 2.

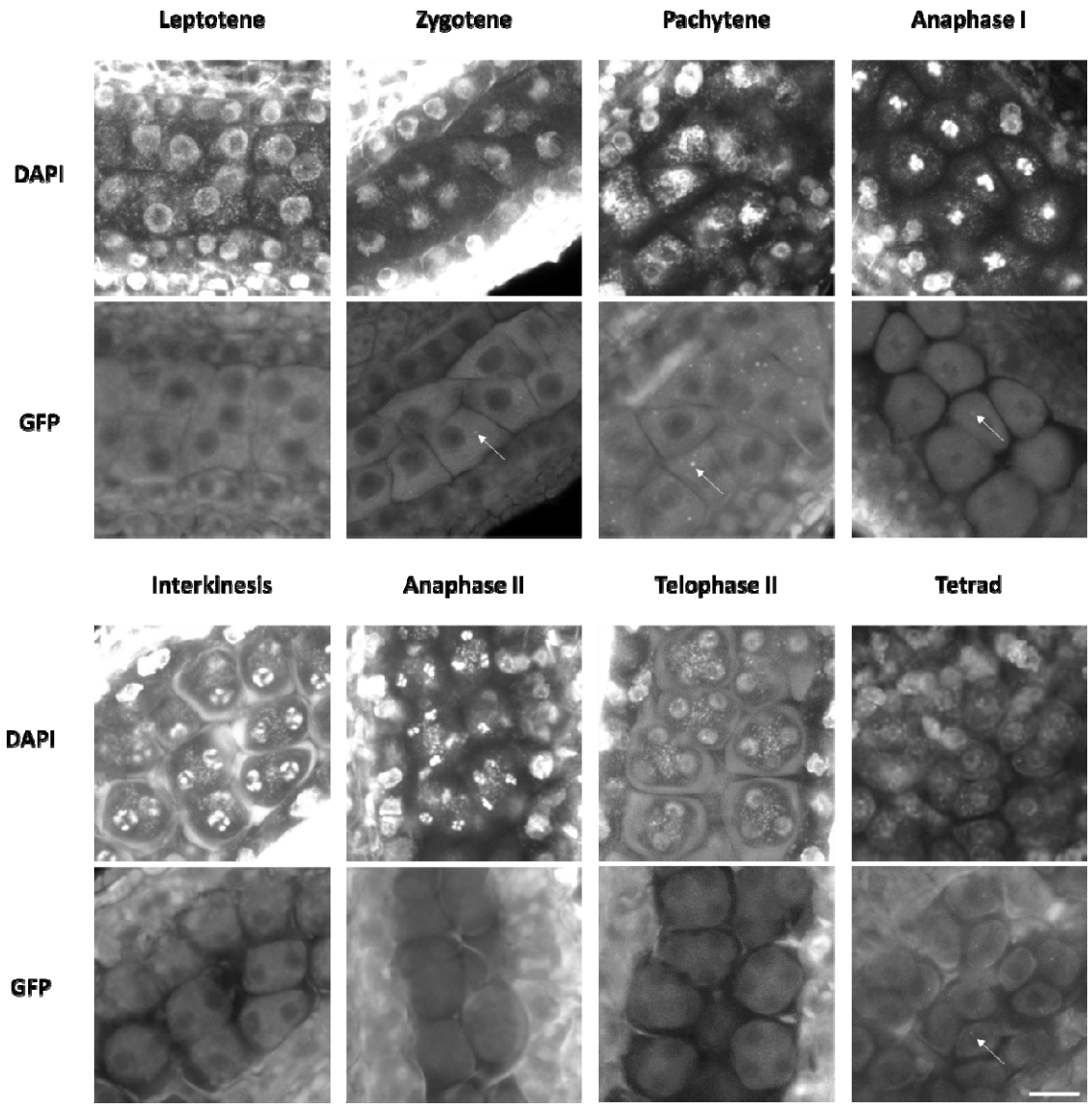
Leptotene
Zygotene
Pachytene
Anaphase I
DAPI
GFP
Interkinesis
Anaphase II
Telophase II
Tetrad
DAPI
GFP

Figure 3 Localisation of TAM-GFP during meiosis.

Confocal images of DAPI and SR2200 stained anthers of lines expressing TAM::TAM-GFP in the tam-1 mutant background at 20°C at various stages of meiosis. Images are representative examples of various lines expressing the Col-0 or Mt-0 allele of TAM. Arrows denote GFP foci. Scale bar = 10µm.

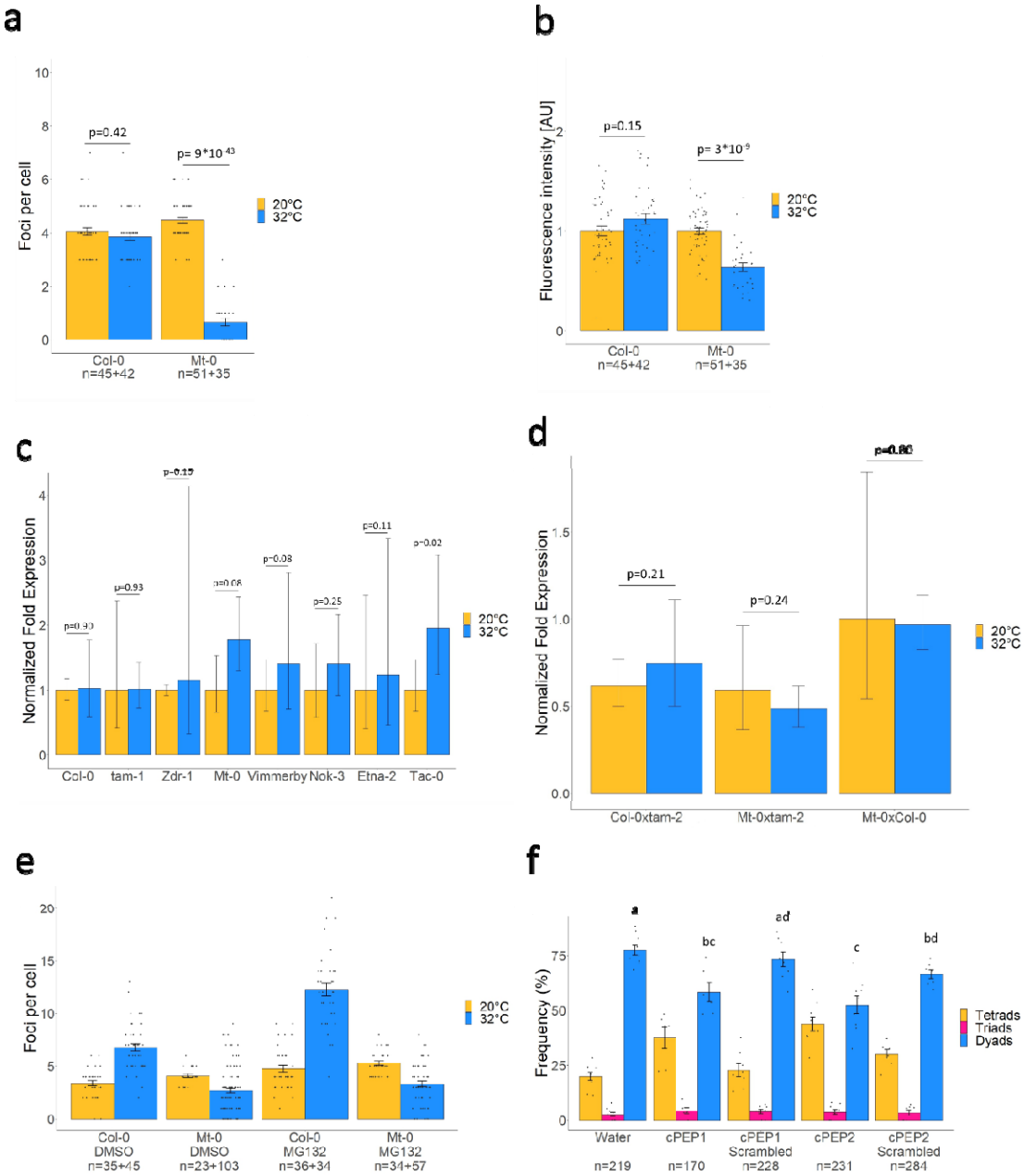
a
Foci per cell
p=0.42
p= 9*10-43
20°C
32°C
Col-0
n=45+42
Mt-0
n=51+35
b
Fluorescence intensity [AU]
p=0.15
p= 3*10-9
20°C
32°C
Col-0
n=45+42
Mt-0
n=51+35
c
Normalized Fold Expression
p=0.93
p=0.15
p=0.08
p=0.08
p=0.25
p=0.11
p=0.02
20°C
32°C
Col-0
tam-1
Zdr-1
Mt-0
Vimmerby
Nok-3
Etna-2
Tac-0
d
Normalized Fold Expression
p=0.21
p=0.24
20°C
32°C
Col-0xtam-2
Mt-0xtam-2
Mt-0xCol-0
e
Foci per cell
20°C
32°C
Col-0
DMSO
n=35+45
Mt-0
DMSO
n=23+103
Col-0
MG132
n=36+34
Mt-0
MG132
n=34+57
f
Frequency (%)
a
bc
ad
c
bd
Tetrads
Triads
Dyads
Water
n=219
cPEP1
n=170
cPEP1
Scrambled
n=228
cPEP2
n=231
cPEP2
Scrambled
n=284

Figure 4 Heat interferes with TAM expression.

a) Quantification of the number of GFP foci in pachytene-diplotene stage anthers of lines carrying the Col-0 or Mt-0 TAM construct at 20°C or after 24h at 32°C. **b)** Quantification of the overall fluorescence intensity in the cytosol of those lines, integrated over the entire cell and normalised to the 20°C control for every line. **c,d)** RT-qPCR based TAM mRNA expression levels from flowerbuds of plants grown at 20°C or after a 24h at 32°C heat treatment. Data are normalized to the 20°C control within each accession **(c)** or to the Mt-0xCol-0 20°C control **(d)**. Three individual plants were analysed per accession and per treatment. p-values correspond to a linear model fit comparing the 20°C control to the 32°C treatment within each accession. Error bars represent standard errors. **e)** Quantification of the number of GFP foci in pachytene-diplotene stage anthers of lines carrying the native TAM constructs of either Col-0 or Mt-0 at 20°C or after 24h at 32°C. Data were collected from *in vitro* propagated inflorescences treated with either MG132 or a DMSO mock. For **a,b** and **f** error bars represent standard errors. The number of individual meiocytes analysed is represented by n = 'number of meiocytes at 20°C' + 'number meiocytes at 32°C' (identical for **a** and **b**), and individual cells are represented by black dots. p-values were Benjamini-Hochberg adjusted for multiple testing, p-values for **(e)** can be found in Supp. Table S3. **f)** Quantification of the frequency of dyads, triads and tetrads at the tetrad-stage of Mt-0 flowerbuds; *in vitro* treated with cPEPs 1 or 2, their respective scrambled versions or a water mock. Error bars represent standard errors. n represents the number of meiocytes counted, individual anthers are represented by black dots. Statistical differences are denoted by compact letter display based on Wilcoxon rank-sum tests on the dyad frequency and Benjamini-Hochberg adjusted for multiple testing.

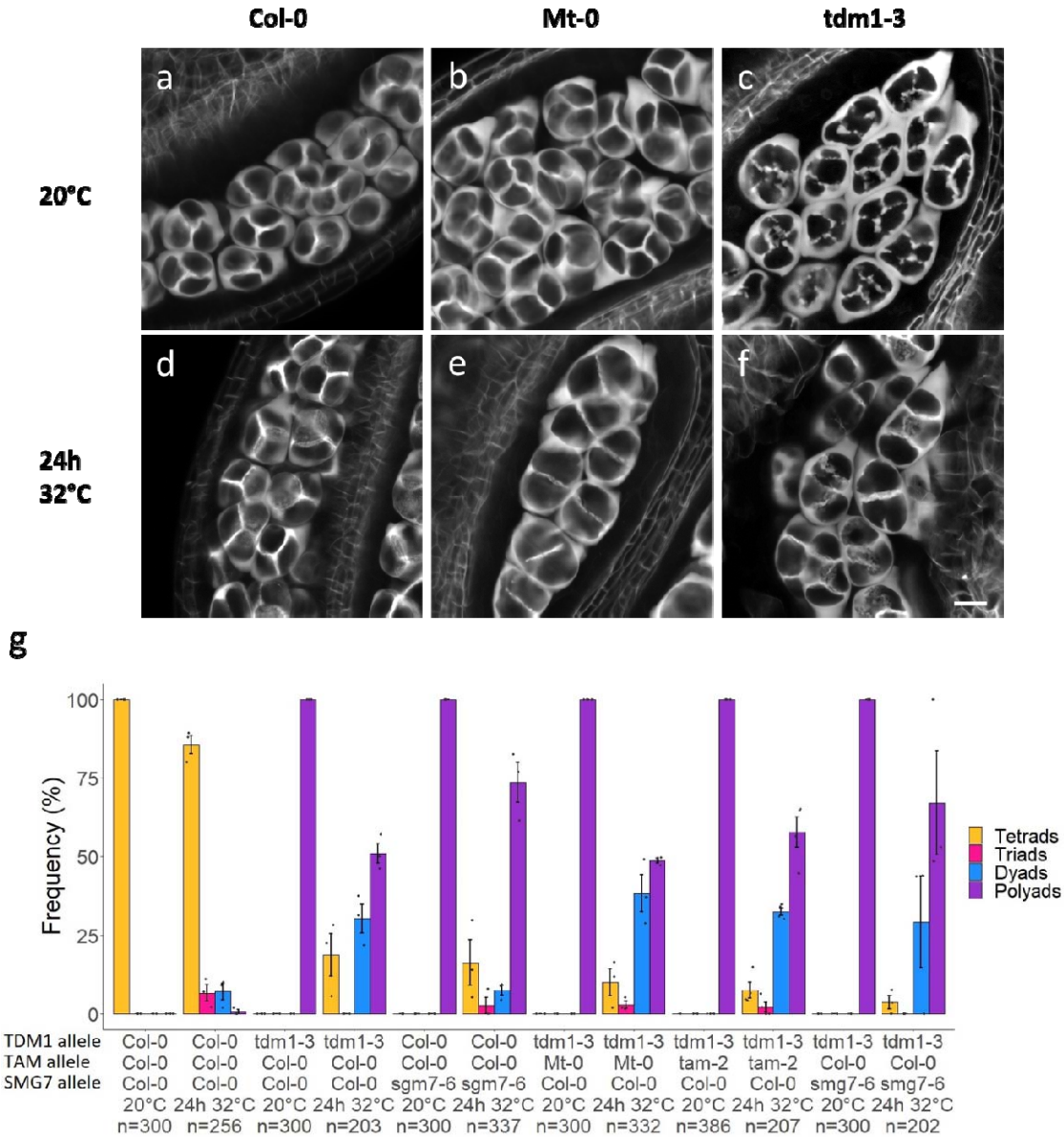
Col-0
Mt-0
tdm1-3
20°C
24h
32°C
a
b
c
d
e
f
g
Frequency (%)
100
75
50
25
0
Tetrads
Triads
Dyads
Polyads
TDM1 allele
TAM allele
SMG7 allele
Col-0 Col-0 Col-0 20°C n=300
Col-0 Col-0 Col-0 24h n=256
tdm1-3 Col-0 Col-0 32°C n=300
tdm1-3 Col-0 Col-0 20°C n=203
Col-0 Col-0 sgm7-6 24h n=300
Col-0 Col-0 sgm7-6 32°C n=337
tdm1-3 Mt-0 Col-0 20°C n=300
tdm1-3 Mt-0 Col-0 24h n=332
tdm1-3 tam-2 Col-0 32°C n=386
tdm1-3 tam-2 Col-0 20°C n=207
tdm1-3 Col-0 smg7-6 24h n=300
tdm1-3 Col-0 smg7-6 32°C n=202

Figure 5 Heat stress rescues meiotic progression mutants.

a-f) Confocal images of SR2200 stained tetrad-stage meiotic anthers of Col-0, Mt-0 or tdm1-3 at 20°C or after 24h at 32°C. Scale bar = 10µm. **i)** Frequencies (%) of tetrads, triads, dyads or polyads at the tetrad-stage of lines carrying various combinations of TAM, TDM1 and SMG7 alleles at 20°C or after 24h at 32°C. Lines were PCR genotyped to ensure homozygosity of the mentioned alleles. n represents the number of individual meiocytes counted. At least 3 plants were analysed for every genotype and treatment, represented by black dots. Error bars represent standard errors.

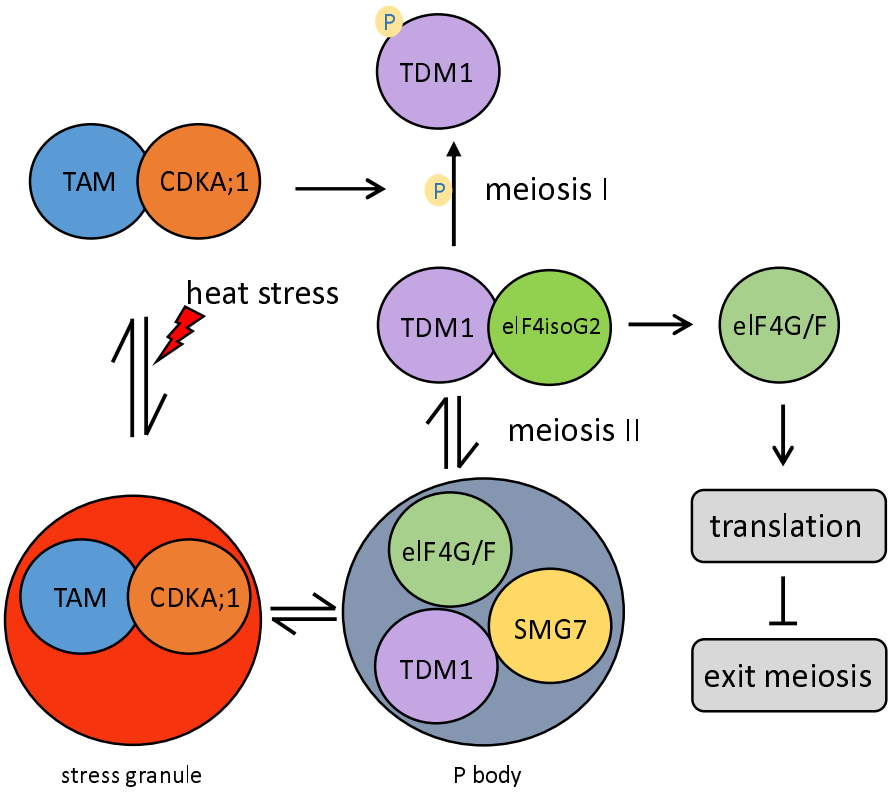
P
TDM1
TAM
CDKA;1
P
meiosis I
heat stress
TDM1
eIF4isoG2
eIF4G/F
meiosis II
translation
TAM
CDKA;1
eIF4G/F
SMG7
TDM1
exit meiosis
stress granule
P body

Figure 6 Model for meiosis exit.

Progression and exit of male meiosis are controlled by the cell cycle regulators TAM and CDKA;1. TDM1 is phosphorylated during meiosis I which prevents it from interaction with protein translation initiation factor elF4isoG2. This allows protein translation and inhibition of meiosis exit. At the end of meiosis II, TDM1 is no longer phosphorylated and gets recruited to P-bodies through interaction with SMG7. Together they bind to elF4G factors and this likely recruits the translation initiation machinery to the P-body. In the absence of translation, meiosis exit takes place. Under heat stress conditions, TAM and CDKA;1 are recruited to stress granules and this hinders TDM1 phosphorylation resulting in recruitment of the translation machinery into P-bodies or possibly also stress granules, resulting in limited translation and meiosis exit.

548

a

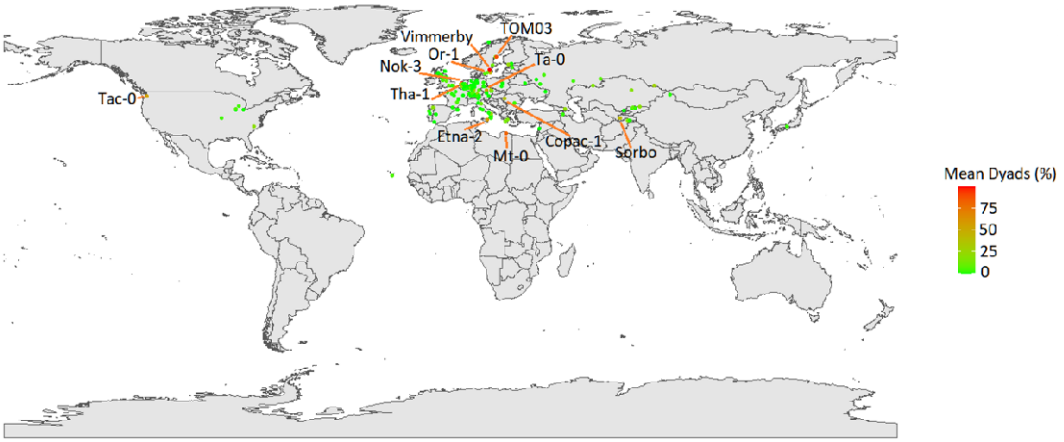

b

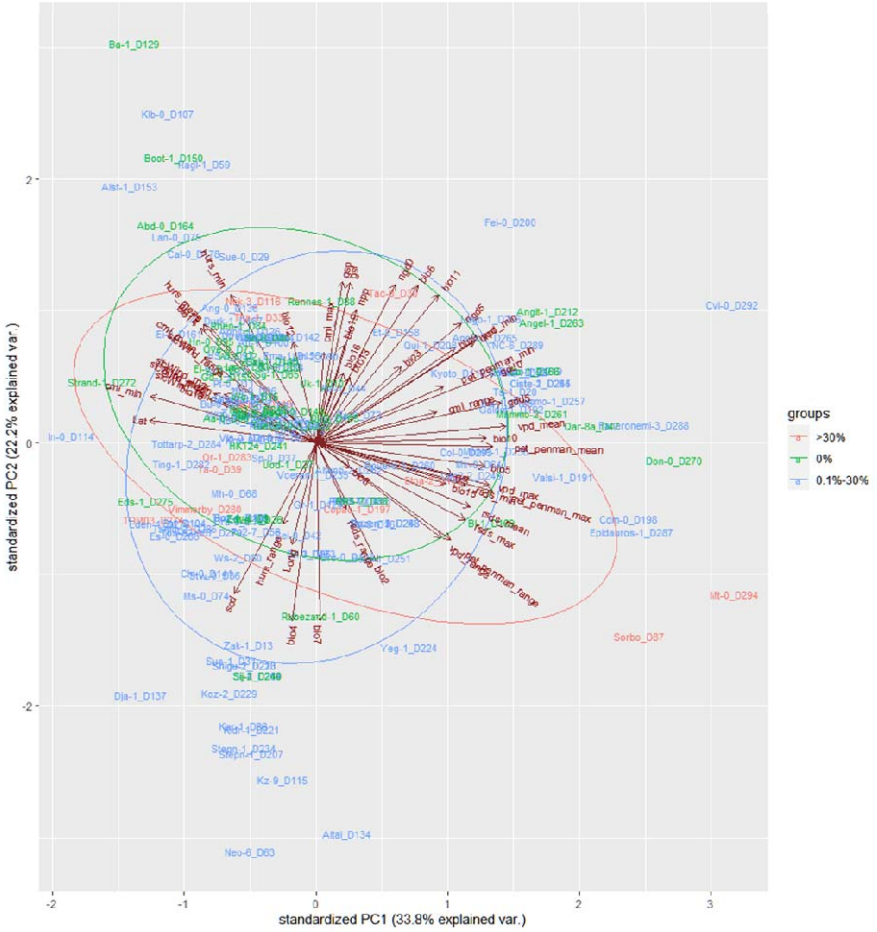

549
550

Supplemental Figure 1 Correlating dyad production frequency with geographical and climatological data.

a) Geographical location of the analysed accessions, coloured according to the average amount of dyads produced at the tetrad-stage after 24h at 32°C. The 11 highest dyad producing accessions are denoted with their name. **b)** Biplot for the principle component analysis of the dyad production frequency of different Arabidopsis accessions heat treated for 24h at 32°C, based on climatological data of the CHELSEA Bioclim dataset (Karger et al., 2017). Accessions are divided into 3 groups based on their average dyad production frequency (>30%, 0.1%-30%, 0%) and coloured accordingly.

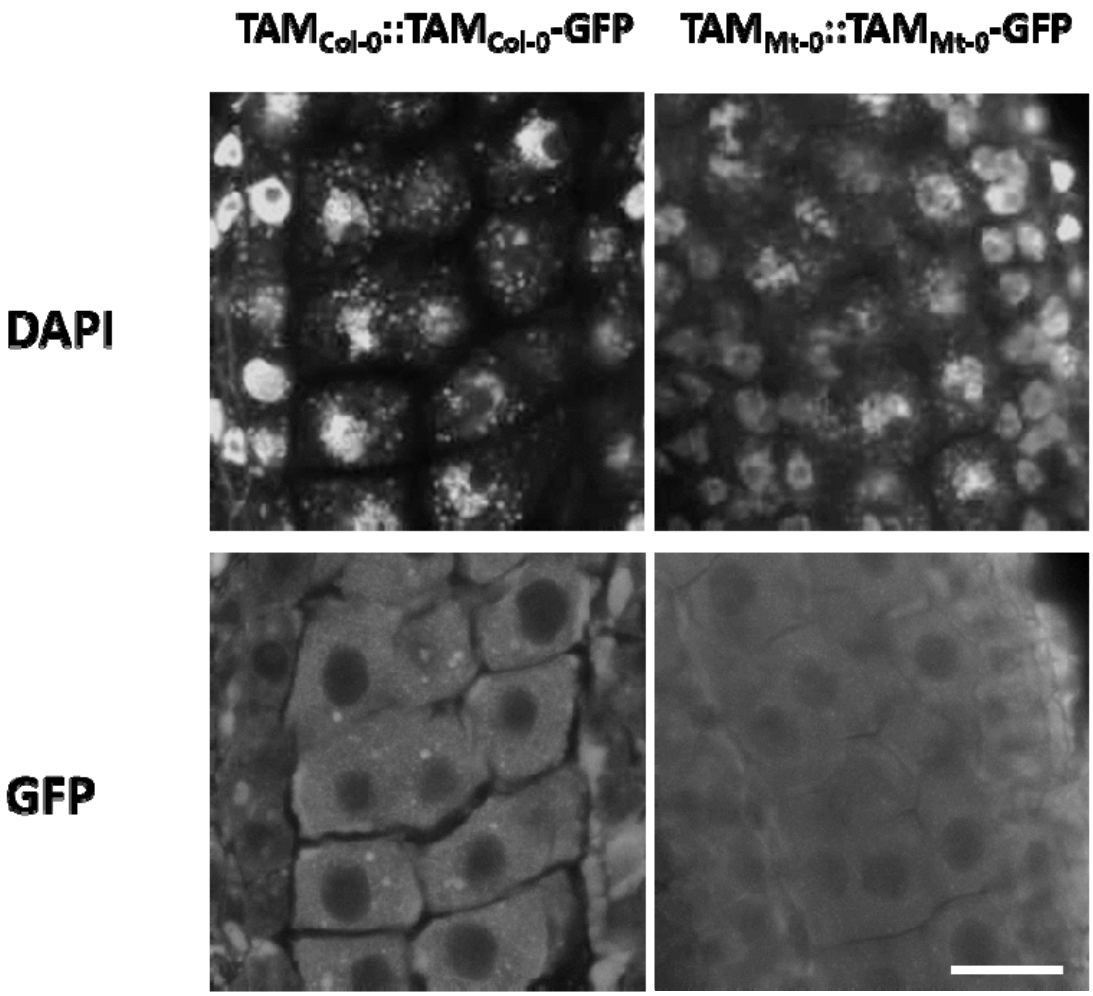
TAMCol-0::TAMCol-0-GFP
TAMMt-0::TAMMt-0-GFP
DAPI
GFP

Supplemental Figure 2 Expression of TAM-GFP at high temperatures.

Confocal images of DAPI and SR2200 stained anthers of lines expressing TAM::TAM-GFP in the tam-1 mutant background at the pachytene-diplotene stage after a 24h treatment at 32°C. Scale bar = 10µm.

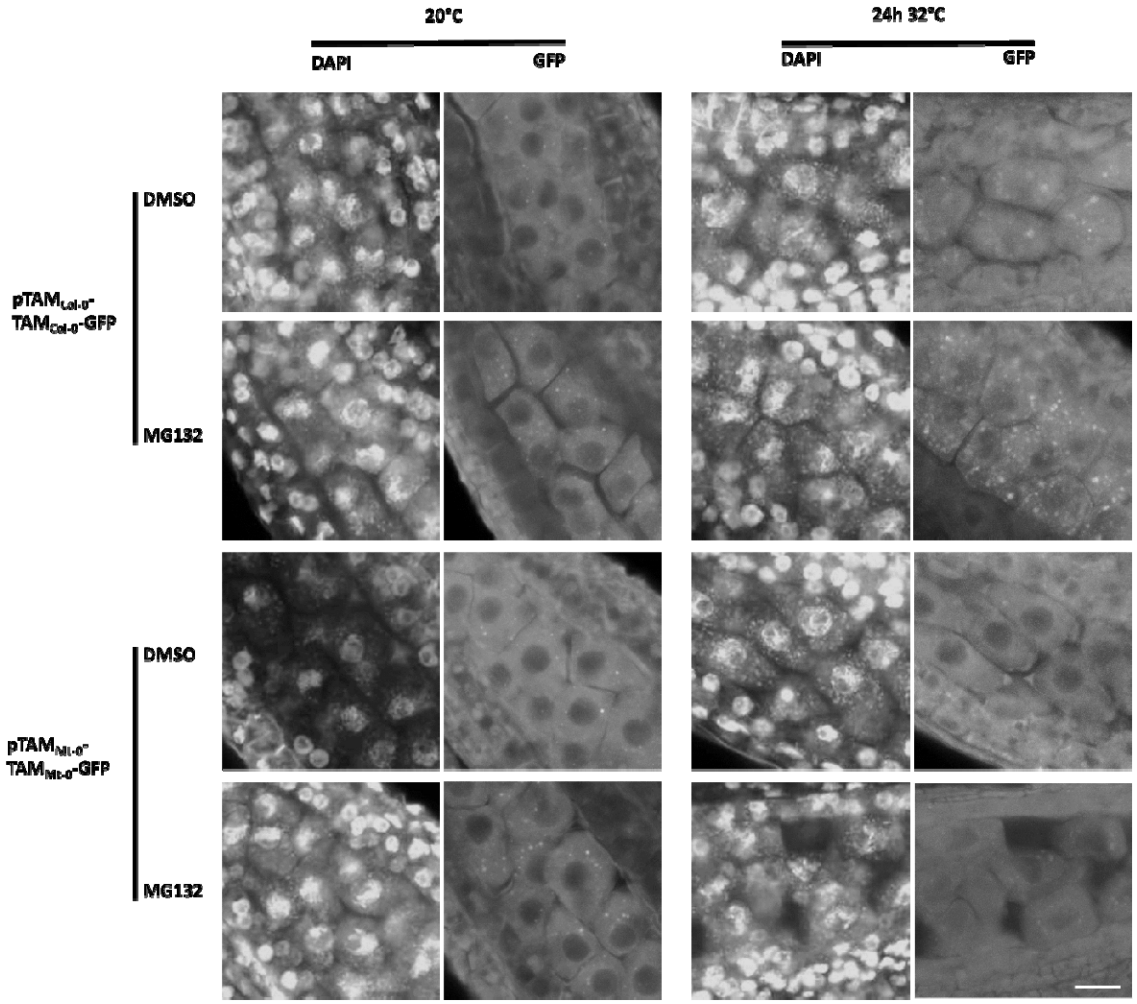
20°C
24h 32°C
DAPI
GFP
DAPI
GFP
DMSO
MG132
pTAM$_{Col-0}$-
TAM$_{Col-0}$-GFP
DMSO
MG132
pTAM$_{Mt-0}$-
TAM$_{Mt-0}$-GFP

Supplemental Figure 3 Confocal images of MG132 treated meiotic anthers at various temperatures.

Confocal images of DAPI and SR2200 stained meiotic anthers at the pachytene-diplotene stage of lines carrying the native Col-0 or Mt-0 TAM construct coupled with GFP in the tam-1 background. Inflorescences were *in vitro* treated with MG132 or a DMSO mock for 24h at 20°C or 32°C. Scale bar = 10µm.

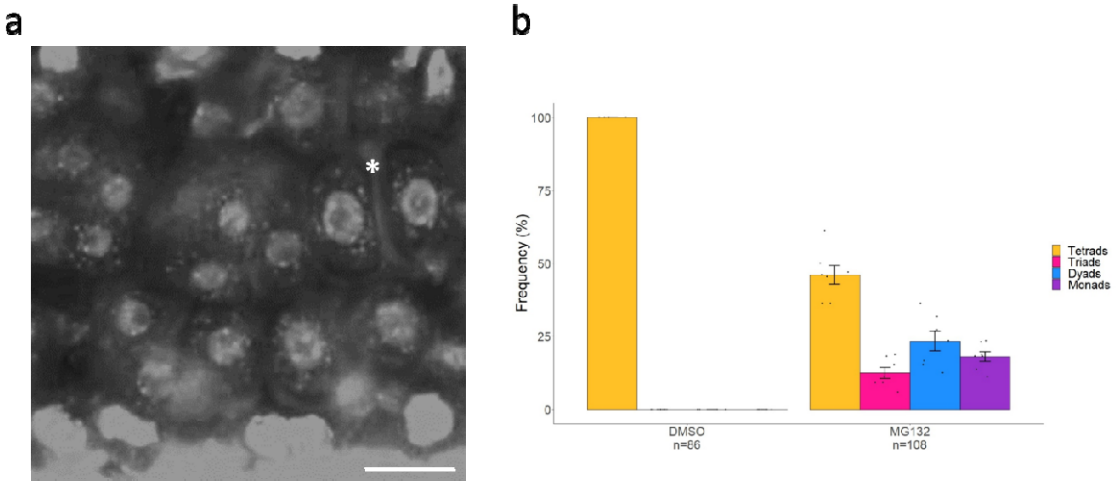
a
b
*
100
75
50
25
0
Frequency (%)
DMSO
n=66
MG132
n=106
Tetrads
Triads
Dyads
Monads

Supplemental Figure 4 MG132 treatment disrupts meiotic progression.

a) Confocal image of a DAPI and SR2200 stained meiotic anther at the tetrad stage of accession tam-1 complemented with the native Col-0 TAM-GFP construct, *in vitro* treated with MG132. The * indicates the presence of a dyad. Scale bar = 10µm. **b)** Quantification of the frequency of tetrads, triads, dyads and monads at the tetrad-stage of the same line, *in vitro* treated with MG132 or a DMSO mock at 20°C. n represents the number of individual meiocytes counted. Error bars represent standard errors of the mean. A minimum of 4 plants were analysed per treatment, individual plants are represented by black dots.

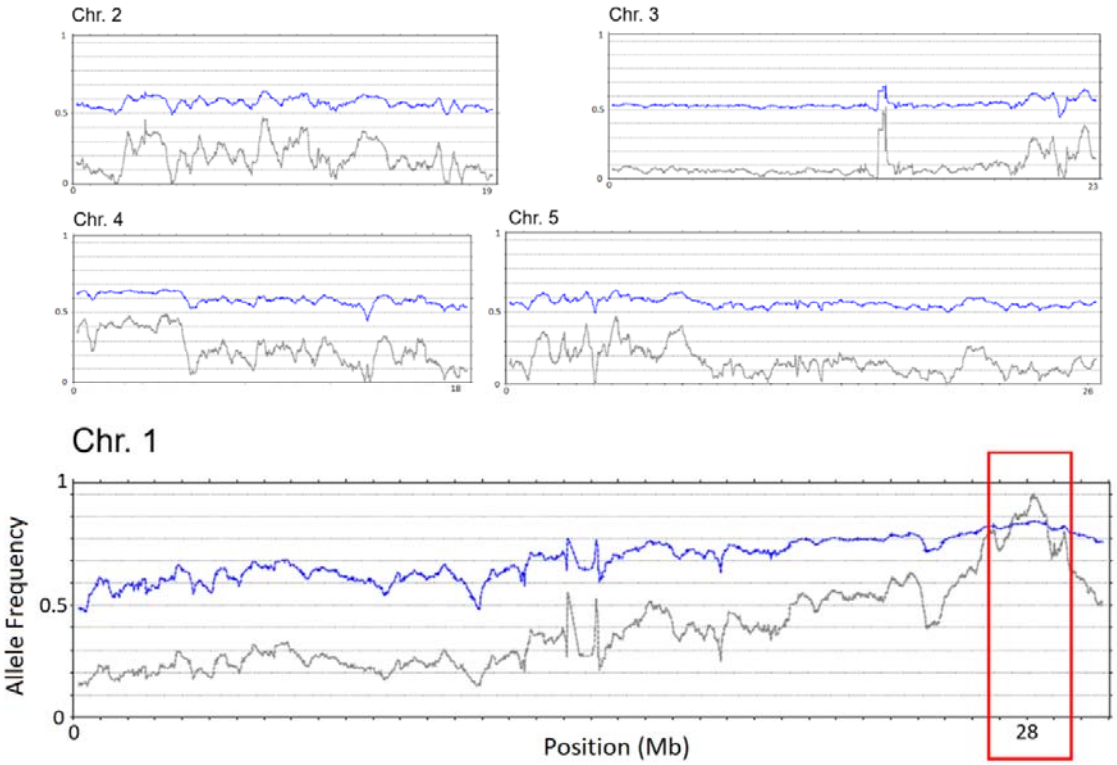
Chr. 2
Chr. 3
Chr. 4
Chr. 5
Chr. 1
Allele Frequency
1
0.5
0
0
28
Position (Mb)

Supplemental Figure 5 The Mt-0 high dyad locus maps to the bottom of chr1.

Allele frequency plot of the mapping population for the high dyad phenotype after heat stress of Mt-0xLer, analysed using SHOREmap V3.0. The blue line shows the average allele frequency within a 400kb window (5kb step size), the grey line follows the boost-values. The red rectangle denotes the predicted 2.4Mbp mapping interval.

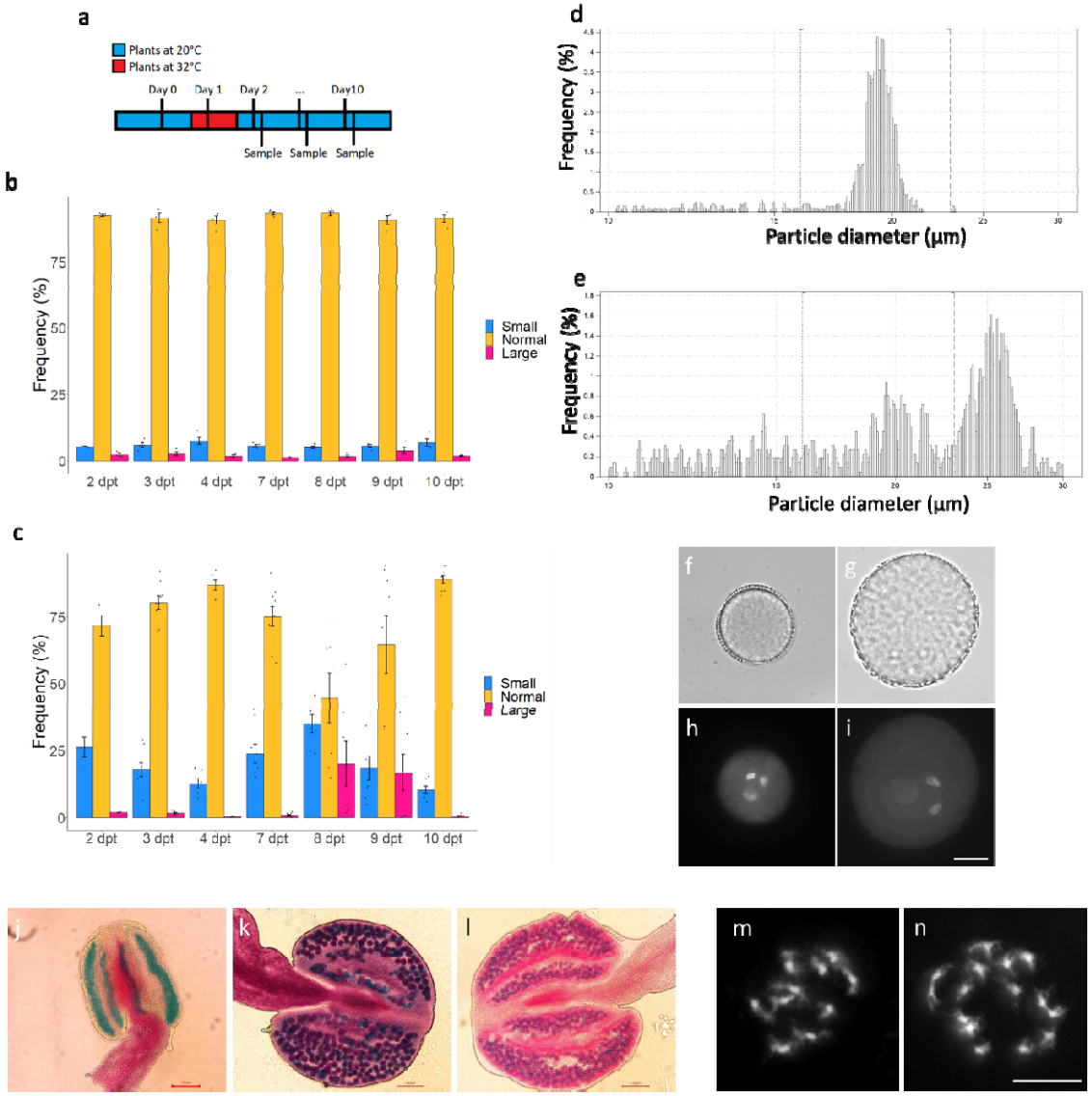
a
Plants at 20°C
Plants at 32°C
Day 0
Day 1
Day 2
...
Day10
Sample
Sample
Sample
b
Frequency (%)
Small
Normal
Large
2 dpt
3 dpt
4 dpt
7 dpt
8 dpt
9 dpt
10 dpt
c
Frequency (%)
Small
Normal
Large
2 dpt
3 dpt
4 dpt
7 dpt
8 dpt
9 dpt
10 dpt
d
Frequency (%)
Particle diameter (µm)
e
Frequency (%)
Particle diameter (µm)
f
g
h
i
j
k
l
m
n

Supplemental Figure 6 Heat induces sexual polyploidisation through 2n pollen.

a) Schematic overview of the 24h at 32°C heat treatment, return to the control condition growth rooms and subsequent flower sampling for Coulter Counter analysis. **b-c)** frequency (%) of small (10µm-16µm), normal (16µm-23µm) and large (23µm-30µm) pollen particles analysed through Coulter Counter analysis on 2-10 dpt for Mt-0 plants kept at control conditions (20°C; **b**) and plants heat treated for 24h at 32°C **(c)**. A minimum of 3 individual plants were analysed for every time point and treatment. Individual flowers are represented by black dots. Error bars represent standard errors. **d-e)** representative example of the pollen particle size distribution of Mt-0 plants kept at control conditions (20°C; **d**) and plants heat treated for 24h at 32°C **(e)**. The vertical dotted and dashed lines mark the particle sizes of 16µm and 23µm respectively. **f-i)** bright-field **(f, g)** and corresponding DAPI stained **(h, i)** images of control (20°C) pollen **(f, h)** and enlarged pollen of Mt-0 on day 9 after a 24h at 32°C heat treatment. Scale bar = 10µm. **j-l)** Alexander stained anthers of Mt-0 on days 3 **(j)**, 8 **(k)** and 10 **(l)** after a 24h at 32°C heat treatment. Scale bar = 100µm. **m-n)** DAPI stained, enzyme digested mitotic chromosome spreads of a diploid (2n=10; **m**) and a triploid (3n=15; **n**) Mt-0 plant after heat treatment and self-fertilization. Scale bar = 10µm. Subpanels **d, e, h, i, m** and **n** are re-used from Figure 1 of the main text to allow for easy comparison.

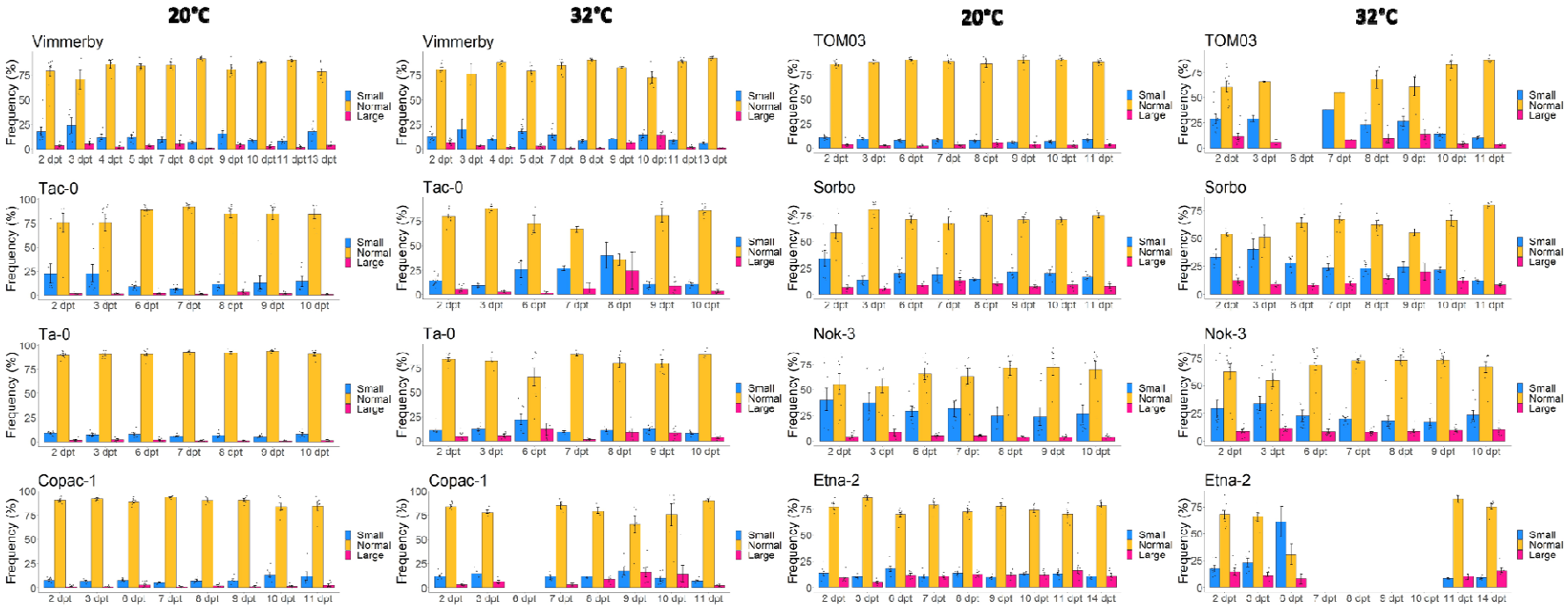
20°C
32°C
20°C
32°C
Vimmerby
Vimmerby
TOM03
TOM03
Tac-0
Tac-0
Sorbo
Sorbo
Ta-0
Ta-0
Nok-3
Nok-3
Copac-1
Copac-1
Etna-2
Etna-2
Frequency (%)
Small
Normal
Large

617

618

Supplemental Figure 7 Pollen particle size time series for 8 temperature sensitive accessions.

Frequency (%) of small (10µm-16µm), normal (16µm-23µm) and large (23µm-30µm) pollen particles analysed through Coulter Counter analysis for plants kept at control conditions (20°C) and plants heat treated for 24h at 32°C for 8 temperature sensitive accessions. A minimum of 3 individual plants were analysed for every time point and treatment. Individual flower measurements are represented by black dots. Error bars represent standard errors. dpt = days after the heat treatment.

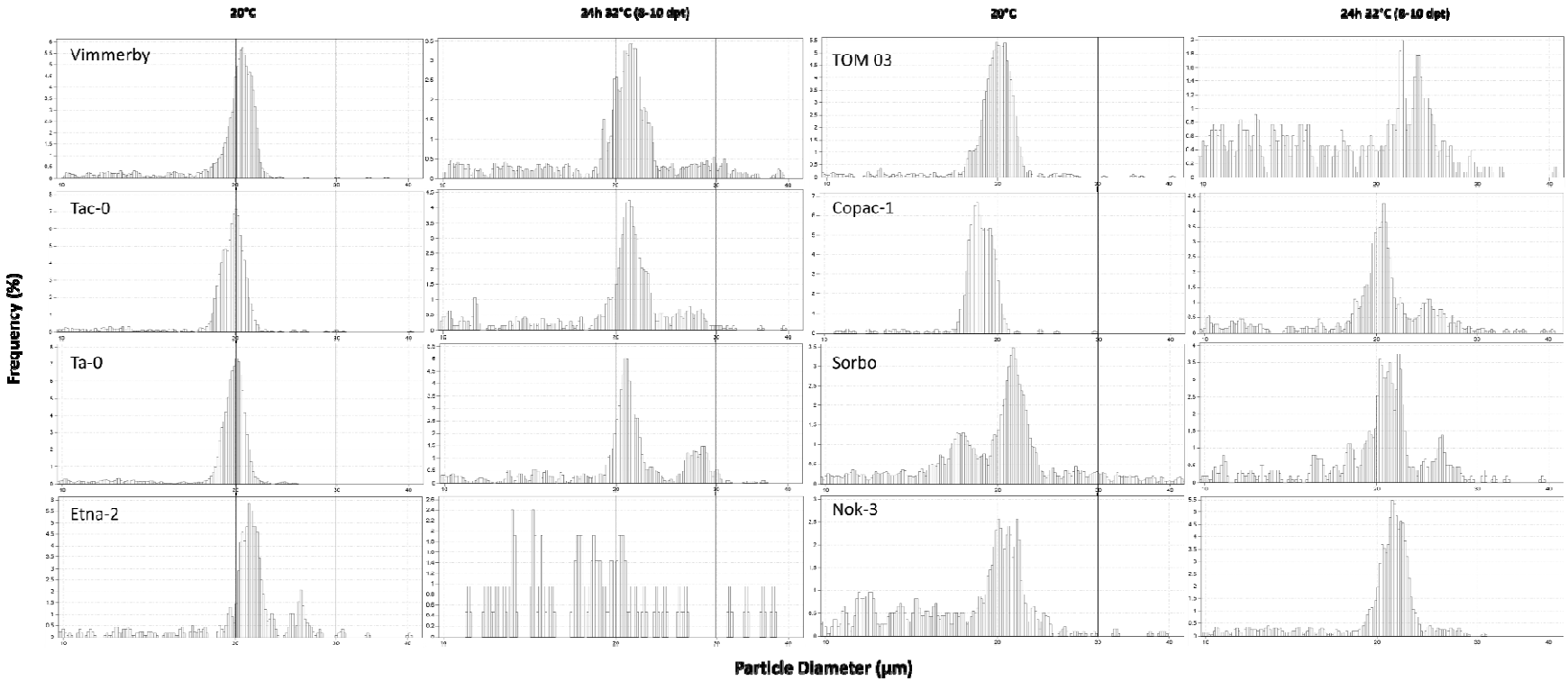
20°C
24h 32°C (8-10 dpt)
20°C
24h 32°C (8-10 dpt)
Vimmerby
TOM 03
Tac-0
Copac-1
Ta-0
Sorbo
Etna-2
Nok-3
Frequency (%)
Particle Diameter (µm)

Supplemental Figure 8 Pollen particle size distribution for 8 temperature sensitive accessions.

Examples of the pollen particle size distributions of 8 temperature sensitive accessions for plants kept at control conditions (20°C) and plants heat treated for 24h at 32°C. The vertical black lines mark the particle sizes of 20µm and 30µm for easy comparison.

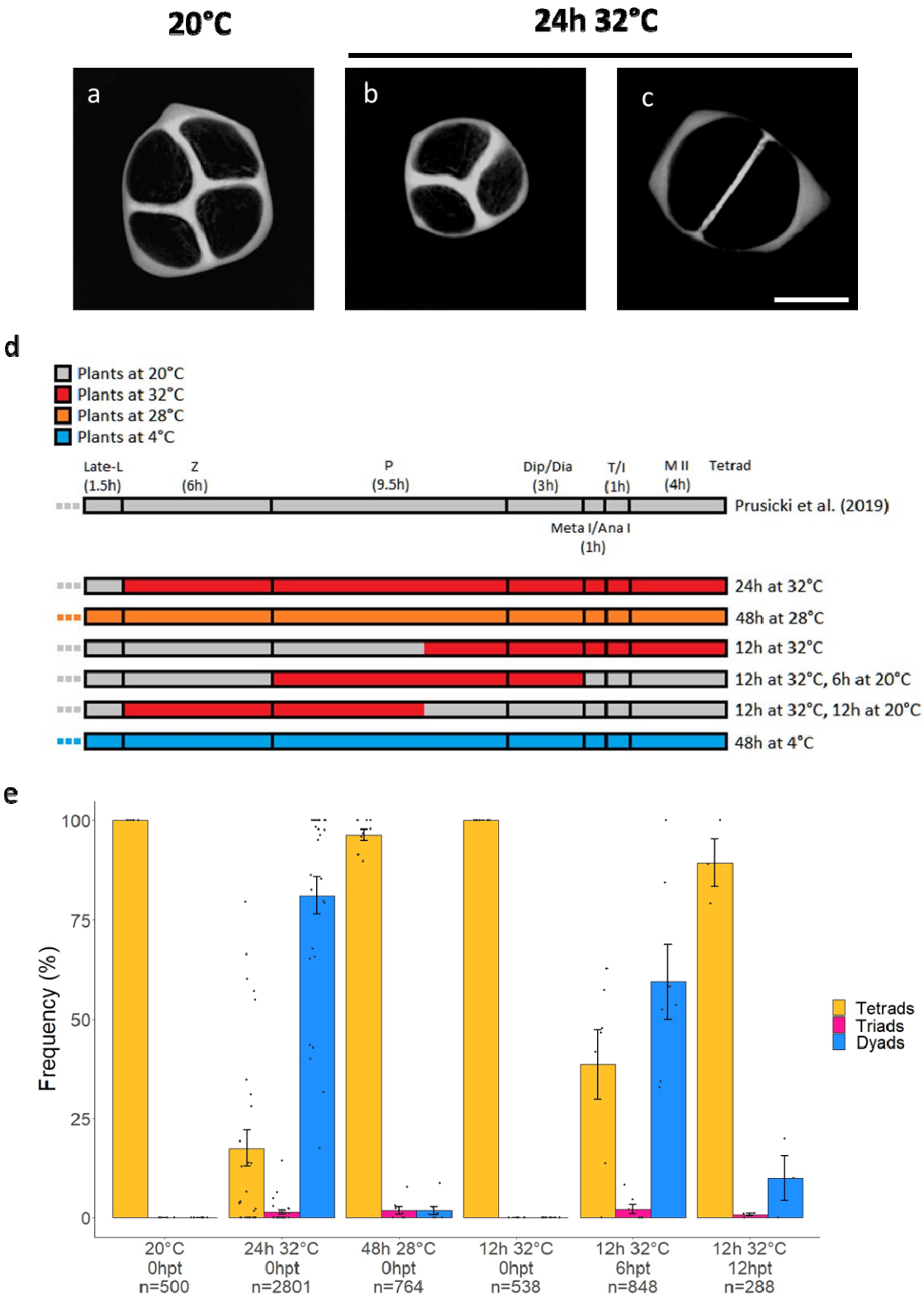
20°C
24h 32°C
a
b
c
d
Plants at 20°C
Plants at 32°C
Plants at 28°C
Plants at 4°C
Late-L (1.5h)
Z (6h)
P (9.5h)
Dip/Dia (3h)
T/I (1h)
M II (4h)
Tetrad
Prusicki et al. (2019)
Meta I/Ana I (1h)
24h at 32°C
48h at 28°C
12h at 32°C
12h at 32°C, 6h at 20°C
12h at 32°C, 12h at 20°C
48h at 4°C
e
Frequency (%)
100
75
50
25
0
Tetrads
Triads
Dyads
20°C 0hpt n=500
24h 32°C 0hpt n=2801
48h 28°C 0hpt n=764
12h 32°C 0hpt n=538
12h 32°C 6hpt n=848
12h 32°C 12hpt n=288

Supplemental Figure 9 Meiotic restitution in Mt-0 at various temperatures.

a-c) Aniline blue stained Mt-0 tetrad-stage male meiocytes under control conditions **(a)** and after a 24h at 32°C heat treatment **(b, c,)**. Scale bar = 10µm. **d)** Schematic overview of the different temperature treatments and durations applied to Mt-0 regarding the timing and progression of male meiosis as described by (Prusicki et al., 2019). **e)** Frequency (%) of the different configurations (tetrads, triads or dyads) observed at the tetrad-stage of Mt-0 after various temperature treatments. n represents the number of individual meiocytes counted. Error bars represent standard errors. A minimum of 3 plants were analysed for every treatment, represented by black dots. For easy comparison, data of Mt-0 at 20°C and for 24h at 32°C was re-used from Figure 2a of the main text.

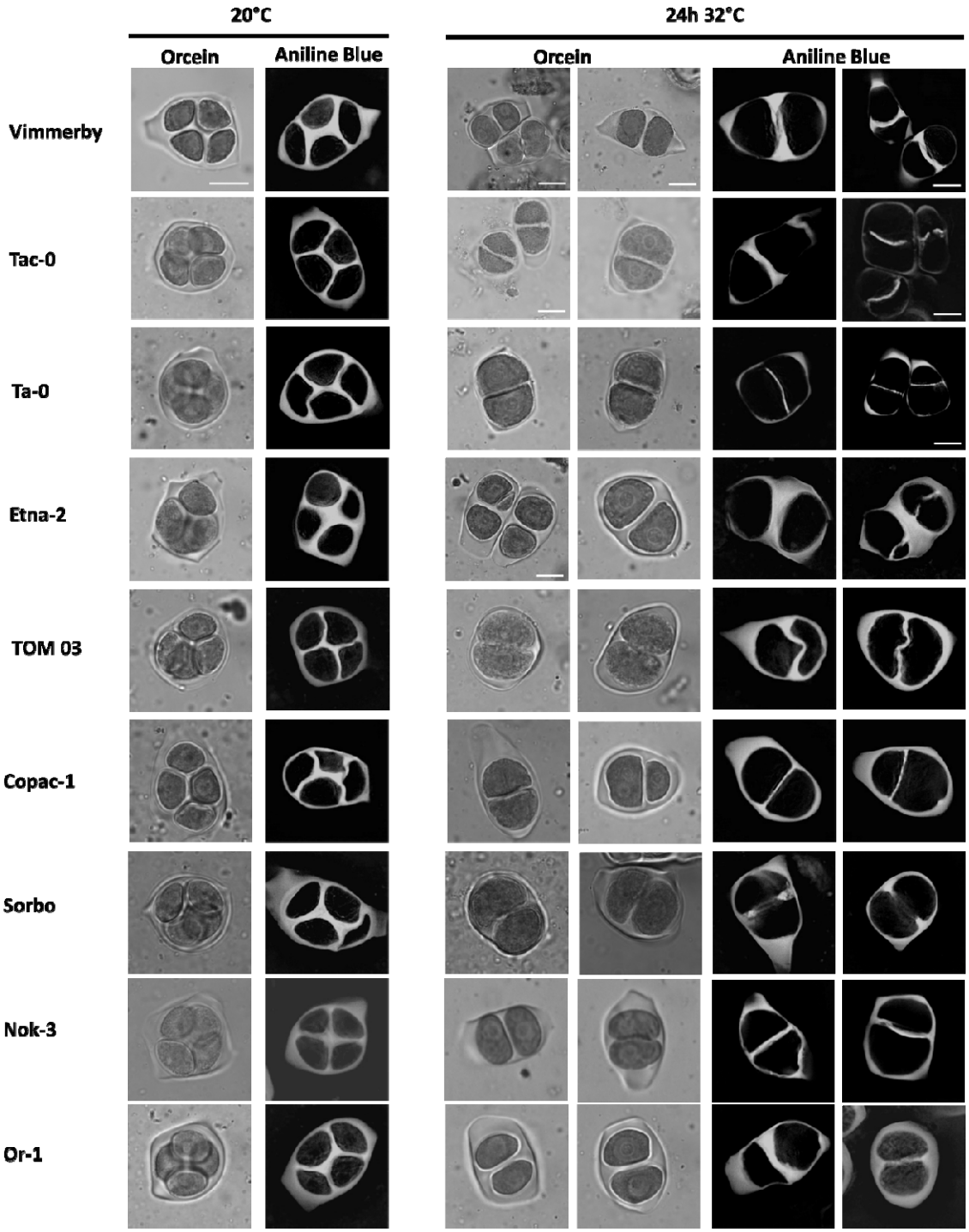
20°C
24h 32°C
Orcein
Aniline Blue
Orcein
Aniline Blue
Vimmerby
Tac-0
Ta-0
Etna-2
TOM 03
Copac-1
Sorbo
Nok-3
Or-1

644
645

Supplemental Figure 10 Temperature sensitive accessions' tetrad stage phenotype.

Representative images of orcein or aniline blue stained tetrad-stage meiotic products of different high frequency, heat induced dyad producing accessions under control conditions (20°C) or immediately after a 24h at 32°C treatment. Scale bar = 10µm.

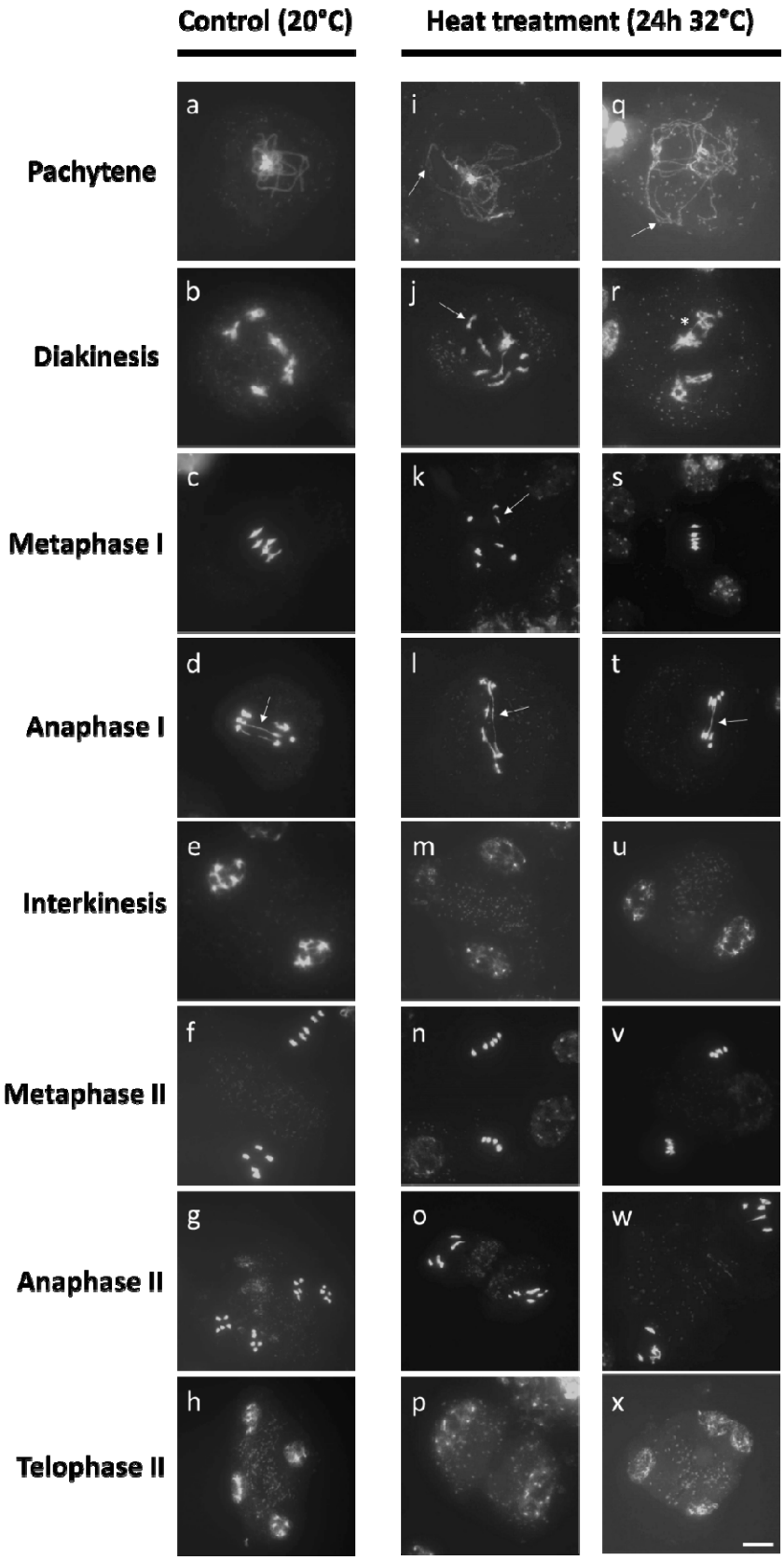
Control (20°C)
Heat treatment (24h 32°C)
Pachytene
Diakinesis
Metaphase I
Anaphase I
Interkinesis
Metaphase II
Anaphase II
Telophase II
a
b
c
d
e
f
g
h
i
j
k
l
m
n
o
p
q
r
s
t
u
v
w
x

651

Supplemental Figure 11 Meiotic spreads of Mt-0.

DAPI stained, enzyme digested chromosome spreads of Mt-0 male meiocytes at various developmental stages under control conditions (20°C; **a-h**) and after a 24h at 32°C heat treatment **(i-x)**. Regions of asynapsis at pachytene, univalents at diakinesis and metaphase I and ectopic chromosome strands at anaphase I are indicated by arrows. Aberrant interactions between non-homologous chromosomes at diakinesis are indicated with an asterix. Scale bar = 10µm.

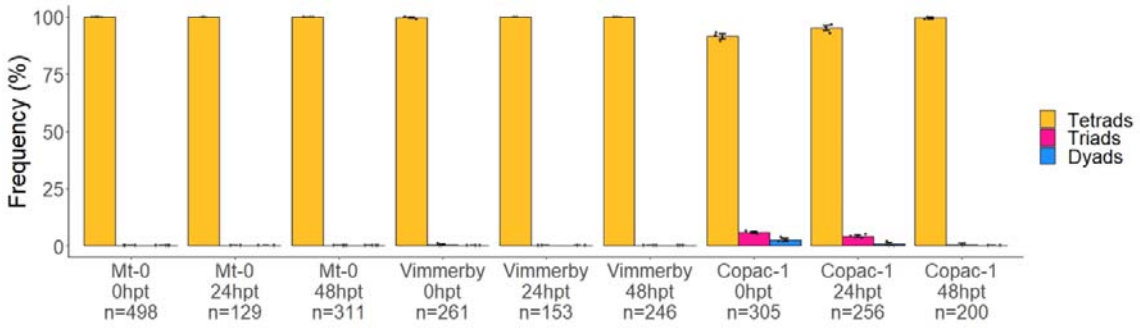
Frequency (%)
100
75
50
25
0
Mt-0 0hpt n=498
Mt-0 24hpt n=129
Mt-0 48hpt n=311
Vimmerby 0hpt n=261
Vimmerby 24hpt n=153
Vimmerby 48hpt n=246
Copac-1 0hpt n=305
Copac-1 24hpt n=256
Copac-1 48hpt n=200
Tetrads
Triads
Dyads

Supplemental Figure 12 The influence of cold on temperature sensitive accessions.

Frequency (%) of the different configurations (tetrads, triads or dyads) observed at the tetrad-stage of 3 high frequency, temperature sensitive accessions (Mt-0, Vimmerby and Copac-1) after a 48h at 4°C cold treatment on 0h, 24h or 48h after the treatment (hpt). Error bars represent standard errors, n represents the number of individual meiocytes counted. Black dots represent the individual plants counted.

ShortName	LongName	Spearman	PVal	PAdjust
gsp	Accumulated precipiation amount on growing season days TREELIM	-0,236	0,002	0,063
gsl	growing season length TREELIM	-0,236	0,002	0,063
bio19	mean monthly precipitation amount of the coldest quarter (kg/m2)	-0,220	0,004	0,063
ngd0	Number of growing degree days	-0,215	0,005	0,063
bio7	annual range of air temperature (°C)	0,211	0,006	0,063
scd	Snow cover days	0,210	0,006	0,063
bio4	temperature seasonality (°C/100)	0,197	0,010	0,091
npp	Net primary productivity	-0,194	0,011	0,091
hurs_min	Minimum monthly nearsurface relative humidity	-0,190	0,013	0,093
cmi_max	Maximum monthly climate moisture index	-0,184	0,016	0,095
rsds_max	Maximum monthly surface downwelling shortwave flux in air	0,182	0,017	0,095
bio12	annual precipitation amount (kg/m^2)	-0,182	0,018	0,095
bio14	precipitation amount of the driest month (kg/m2)	-0,173	0,024	0,112
bio17	mean monthly precipitation amount of the driest quarter (kg/m2)	-0,172	0,025	0,112
bio6	mean daily minimum air temperature of the coldest month (°C)	-0,171	0,026	0,112
gddlgd5	Last growing degree day above 5°C	-0,170	0,044	0,176
bio11	mean daily mean air temperatures of the coldest quarter (°C)	-0,152	0,048	0,181
ngd5	Number of growing degree days	-0,143	0,064	0,226
bio9	mean daily mean air temperatures of the driest quarter (°C)	-0,138	0,072	0,244
bio16	mean monthly precipitation amount of the wettest quarter (kg/m2)	-0,128	0,097	0,287
fcf	Frost change frequency	0,156	0,099	0,287
gdgfgd10	First growing degree day above 10°C	0,130	0,099	0,287
cmi_mean	Mean monthly climate moisture index	-0,122	0,113	0,305
hurs_mean	Mean monthly near-surface relative humidity	-0,122	0,114	0,305
cmi_min	Minimum monthly climate moisture index	-0,119	0,121	0,310
bio2	mean diurnal air temperature range (°C)	0,117	0,129	0,316
vpd_min	Minimum monthly vapor pressure deficit	-0,115	0,134	0,318
gst	Mean temperature of the growing season TREELIM	0,114	0,140	0,319
fgd	first day of the growing season TREELIM	-0,132	0,160	0,337
rsds_range	Annual range of monthly surface downwelling shortwave flux in air	0,108	0,162	0,337
bio15	precipitation seasonality (kg/m2)	0,107	0,163	0,337
bio3	isothermality (°C)	-0,106	0,168	0,337
pet_penman_min	Minimum monthly potential evapotranspiration	-0,102	0,186	0,359
rsds_mean	Mean monthly surface downwelling shortwave flux in air	0,101	0,191	0,359
bio13	precipitation amount of the wettest month (kg/m2)	-0,096	0,212	0,371
gdd0	Growing degree days heat sum above 0°C	-0,096	0,212	0,371
bio1	mean annual air temperature (°C)	-0,096	0,215	0,371
ngd10	Number of growing degree days	-0,084	0,277	0,467
pet_penman_range	Annual range of monthly potential evapotranspiration	0,081	0,292	0,480
hurs_range	Annual range of monthly nearsurface relative humidity	0,080	0,301	0,482
gdd5	Growing degree days heat sum above 5°C	-0,076	0,323	0,504
lgd	last day of the growing season TREELIM	-0,088	0,348	0,519
rsds_min	Minimum monthly surface downwelling shortwave flux in air	0,072	0,352	0,519
sfcWind_range	Annual range of monthly near-surface wind speed	-0,071	0,360	0,519
gdgfgd5	First growing degree day above 5°C	0,077	0,366	0,519
sfcWind_max	Maximum monthly nearsurface wind speed	-0,068	0,380	0,519
gddlgd10	Last growing degree day above 10°C	-0,069	0,381	0,519
sfcWind_min	Minimum monthly nearsurface wind speed	-0,058	0,454	0,604
sfcWind_mean	Mean monthly near-surface wind speed	-0,056	0,469	0,604
hurs_max	Maximum monthly nearsurface relative humidity	-0,053	0,489	0,604
vpd_range	Annual range of monthly vapor pressure deficit	0,053	0,493	0,604
bio18	mean monthly precipitation amount of the warmest quarter (kg/m2)	-0,051	0,509	0,604
pet_penman_max	Maximum monthly potential evapotranspiration	0,051	0,509	0,604
gddlgd0	Last growing degree day above 0°C	0,078	0,510	0,604
gdd10	Growing degree days heat sum above 10°C	-0,045	0,559	0,650
gdgfgd0	First growing degree day above 0°C	0,062	0,601	0,687
vpd_mean	Mean monthly vapor pressure deficit	-0,035	0,646	0,725
bio10	mean daily mean air temperatures of the warmest quarter (°C)	-0,031	0,691	0,759
bio8	mean daily mean air temperatures of the wettest quarter (°C)	-0,030	0,700	0,759
swe	Snow water equivalent	-0,033	0,782	0,834
cmi_range	Annual range of monthly climate moisture index	0,014	0,857	0,899
vpd_max	Maximum monthly vapor pressure deficit	0,004	0,954	0,974
bio5	mean daily maximum air temperature of the warmest month (°C)	-0,004	0,959	0,974
pet_penman_mean	Mean monthly potential evapotranspiration	0,001	0,990	0,990

Supplemental Table 1 Correlation of climate variables with the dyad production frequency.

Climate variables of CHELSA Bioclim [29] correlated with the mean dyad frequency after 24h at 32°C for all Arabidopsis accessions analysed. Correlations are based on the Spearman correlation and p-values are presented as original and Benjamini-Hochberg adjusted.

F1 cross	Dyads_Mean (%)	Dyads_SD (%)	n
Mt-0xNok-3	97,5	6,0	274
Etna-2xVimmerby	96,8	5,3	255
Mt-0xTac-0	93,3	6,6	390
Ta-0xVimmerby	92,6	5,7	259
Tac-0xVimmerby	91,5	13,9	244
Mt-0xVimmerby	75,9	46,8	369
Mt-0xTa-0	73,2	16,6	200
Mt-0xOr-1	69,1	29,3	368
Ta-0xTac-0	62,4	34,7	328
Mt-0xEtna-2	60,9	-	64
Mt-0xTha-1	50,0	3,5	394
LerxVimmerby	8,7	6,3	331
LerxTac-0	6,1	10,3	483
LerxTha-1	5,0	3,5	369
LerxTa-0	4,5	4,2	197
Mt-0xLer	3,4	2,9	207
LerxNok-3	1,0	2,1	197
LerxEtna-2	1,0	1,0	284
LerxOr-1	0,5	0,6	577

Supplemental Table 2 Quantification and sample sizes for Figure 2b.

Dyad frequency at the tetrad-stage after 24h at 32°C for different F1 hybrids between several high dyad producing accessions and the Mt-0 and Ler tester lines. Crosses are represented as 'female parent' x 'male parent'. A minimum of 3 heterozygous F1 hybrids were analysed per cross, except for Mt-0xEtna-2 for which only 1 plant was available. SD stands for standard deviation and n represents the number of individual meiocytes counted.

	Col-0 DMSO 20°C	Col-0 DMSO 32°C	Col-0 MG132 20°C	Col-0 MG132 32°C	Mt-0 DMSO 20°C	Mt-0 DMSO 32°C	Mt-0 MG132 20°C
Col-0 DMSO 32°C	**1,20E-11**	-	-	-	-	-	-
Col-0 MG132 20°C	**8,63E-03**	**4,24E-05**	-	-	-	-	-
Col-0 MG132 32°C	**3,83E-49**	**1,66E-25**	**1,29E-38**	-	-	-	-
Mt-0 DMSO 20°C	2,32E-01	**2,13E-06**	2,58E-01	**1,46E-36**	-	-	-
Mt-0 DMSO 32°C	1,21E-01	**2,19E-23**	**1,65E-06**	**5,13E-71**	**6,31E-03**	-	-
Mt-0 MG132 20°C	**3,11E-04**	**3,27E-03**	2,92E-01	**9,80E-34**	**4,61E-02**	**3,00E-09**	-
Mt-0 MG132 32°C	9,33E-01	**1,39E-14**	**2,85E-03**	**2,39E-57**	1,73E-01	8,27E-02	**4,24E-05**

Supplemental Table 3 p-values for Figure 4e.

Benjamini-Hochberg adjusted p-values for the pairwise comparisons of the quantifications in Figure 3e. Values significant on the 5% significance level are presented in bold.

Name	Sequence	Purpose
TAM_WGS_F3	CATCACCCATTGCG TGAGAG	Genotyping tam-1
TAM_WGS_R3	AATCCTGGTTCATTAAGGCAA G	Genotyping tam-1
tam-2(SAIL)_LP	GACTTGATGGATCCACAGC	Genotyping tam-2
tam-2(SAIL)_RP	CAGAAATCCTCCACTTGCG	Genotyping tam-2
tdm1-3_LP	AGCTTCTGGCTTTTTCGATTC	Genotyping tdm1-3
tdm1-3_RP	CCTTACGTCAGAGCCAAACAC	Genotyping tdm1-3
EF1aA4-qRT-F	AGGCTGGTATCTCTAAGGATGGTCA	qPCR
EF1aA4-qRT-R	GGATTTTGTCAGGGTTGTATCCG	qPCR
TAM_qPCR_F	ACTCTCATCTGATGTGGTTGC	qPCR
TAM_qPCR_R(rvc)	AAAGCTCTTGCGGTAGTGAC	qPCR
pTAM_gDNAPromotorR4R1_F	GGGGACAACTTTGTATAGAAAAGTTGTAagagttagagcacgcggtg	Promotor Cloning
pTAM_gDNAPromotorR4R1_R	GGGGACTGCTTTTTTGTACAAACTTGTgttttctttgattagggttttctatttatatttattataagaa	Promotor Cloning
pTAM_gDNAPromotorR4R1_R_Mt-0SNPs	GGGGACTGCTTTTTTGTACAAACTTGTgttttctttgattagggttttctttttttctatttattataagaa	Promotor Cloning (Mt-0 specific)
pTAM_gDNAPromotorR4R1_F_Nok-3_Tac-0SNPs	GGGGACAACTTTGTATAGAAAAGTTGTAagggttacagcacgcggtg	Promotor Cloning (Nok-3 and Tac-0 specific)
TAM_gDNA5'UTR_R1R2_F	GGGGACAAGTTTGTACAAAAAAGCAGGCTTAaaaataattccgcgtttttcattttccgt	mRNA region Cloning
TAM_gDNAR1R2_noSTOP_R	GGGGACCACTTTGTACAAGAAAGCTGGGTTgaggaaaagctcttgcggtagtg	mRNA region Cloning
TAM_gDNA5'UTR_R1R2_F_Mt-0	GGGGACAAGTTTGTACAAAAAAGCAGGCTTAaaaatgattccgcgtttttcattttccgt	mRNA region Cloning (Mt-0 specific)
TAMcPEP1	EDTELLQSDD	Flowerbud treatment
TAMcPEP1 Scrambled	DEDESLDTQL	Flowerbud treatment
TAMcPEP2	DNTYLRNELL	Flowerbud treatment
TAMcPEP2 Scrambled	NYLDERLTNL	Flowerbud treatment

Supplemental Table 4 Primers and peptides used in this study.

	<5% dyads	>>5% dyads	Total
Observed	730	201	931
Expected (1:3)	698	233	931
chi-squared	5,77		
df	1		
p-value	0,016		

Supplemental Table 5 Analysis of the segregation pattern of the Mt-0 locus.

Observed and expected number of individual plants for a 1:3 ratio of low (<5%) vs high (>>5%) heat-induced dyads at the tetrad-stage of a segregating F2 population of a cross between Mt-0 and Ler. The chi-squared value, degrees of freedom (df) and p-value correspond to a goodness-of-fit test between the observed and expected values.

Female Parent	Male Parent	8dpt			9dpt		
		2n	3n	Germ	2n	3n	Germ
Mt-0 (24h 32°C; Selfed)		2	8	10/33	1	4	5/50
Mt-0 (24h 32°C)	Mt-0 (20°C)	17	0	17/51	44	0	44/51
Mt-0 (20°C)	Mt-0 (24h 32°C)	77	0	77/102	64	15	79/102

Supplemental Table 6 Triploid offspring after heat in accession Mt-0.

The number of diploid (2n) and triploid (3n) plants recorded through flow cytometric analysis coming from a cross whereby Mt-0 after a 24h at 32°C heat treatment was either selfed, or used as the male or female parent in a cross with Mt-0 kept at 20°C. Seeds were harvested on siliques that were pollinated 8 or 9 days after the treatment (dpt). ‘Germ’ denotes the ratio of germinated on sown seeds.

	n		Normal		Sturdy		Thin	
	20°C	24h 32°C	20°C	24h 32°C	20°C	24h 32°C	20°C	24h 32°C
Mt-0	21	34	**21**	9	0	0	0	**25**
Vimmerby	19	35	**19**	2	0	**33**	0	0
Etna-2	7	16	**6**	1	1	**13**	0	2
Tac-0	40	27	**40**	1	0	9	0	**17**
Ta-0	12	30	**12**	0	0	0	0	**30**
TOM03	33	29	**33**	2	0	**27**	0	0
Copac-1	23	58	**23**	5	0	0	0	**53**
Sorbo	33	14	**33**	0	0	0	0	**14**
Nok-3	26	8	**26**	1	0	0	0	**7**
Or-1	26	32	**26**	6	0	**15**	0	11

Supplemental Table 7 Quantification of callose wall phenotypes for multiple accessions. Counts of the number of dyads (after 24h at 32°C) or tetrads (after 20°C) having callose walls of normal, sturdy or thin thickness (based on visual inspection of aniline blue stained meiocytes) of several high frequency, heat induced dyad producing accessions. Major fractions are denoted in bold. n represents the number of individual tetrads or dyads counted.

	1 Nucleus	2 Nuclei	More
Mt-0	34	0	0
Vimmerby	41	15	0
Ta-0	26	6	0
Tac-0	17	1	0
Or-1	50	0	0
Etna-2	30	4	0
TOM03	35	7	0
Copac-1	17	15	0
Sorbo	10	14	0
Nok-3	3	11	0

Supplemental Table 8 Quantifications of nuclei per cell at the tetrad stage. Counts of the number of cells containing 1, 2 or more nuclei in dyads of several high frequency, heat induced dyad producing accessions (based on visual inspection of orcein stained meiocytes) after 24h at 32°C. Both cells in a dyad were counted separately.

	Balanced	Unbalanced
Mt-0	51	0
Vimmerby	63	0
Ta-0	38	8
Tac-0	33	3
Or-1	57	0
Etna-2	33	0
TOM03	50	0
Copac-1	39	57
Sorbo	22	4
Nok-3	14	1

Supplemental Table 9 Quantification of balanced and unbalanced meiocytes at the tetrad stage.

Counts of the number of balanced and unbalanced dyads after 24h at 32°C for several high frequency, heat induced dyad producing accessions. In a balanced dyad the 2 cells appear to be equal size, in an unbalanced dyad 1 of the cells is a lot larger than the other (based on visual inspection of aniline blue and orcein stained meiocytes).

Supplemental File 1 Information on the 172 accessions retained for analysis in the tetrad-stage screen after 24h at 32°C (HS).

Including geographical location (Lat and Long), treatment batch (G1-G54), the number of plants analysed (n) and the mean frequency and standard deviation (SD) of dyad, triad and tetrad production. Ranked according to mean dyad production.

Supplemental File 2 Tabular overview of the SNPs of the TAM/CYCA1;2 locus for multiple accessions.

Frequency of SNPs and indels at genomic positions of the TAM/CYCA1;2 locus (chr1: 29081654..29085477) for 8 high frequency, heat induced dyad producing accessions (Vimmerby, Nok-3, Etna-2, Tac-0, Ta-0, Or-1, Tha-1, Mt-0) and for 12 of the lowest frequency dyad producing accessions (Col-0, Ler-0, Litva, Zdr-1, Angit-1, RRS-7, Angel-1, Di-G, Bsch-0, Uod-1, Gel-1, Tol-0). Ranked according to the rarity of the SNPs and indels. Positions with a SNP/indel frequency <= 50 in any of the 8 high dyad producing accessions are coloured yellow and information is added on the genomic location and the consequence of the SNP/indel. SNP/indel data were obtained from https://tools.1001genomes.org/polymorph/ (Alonso-Blanco et al. 2016) or our own resequencing data in case of Mt-0.

Supplemental File 3 Multiple sequence alignment of the TAM/CYCA1;2 genomic sequence.

Multiple sequence alignment of the TAM/CYCA1;2 genomic sequence (chr1: 29081654..29085477) for 8 high frequency, heat induced dyad producing accessions (Vimmerby, Nok-3, Etna-2, Tac-0, Ta-0, Or-1, Tha-1, Mt-0) and for 12 of the lowest frequency dyad producing accessions (Col-0, Ler-0, Litva, Zdr-1, Angit-1, RRS-7, Angel-1, Di-G, Bsch-0, Uod-1, Gel-1, Tol-0).

Supplementary Note 1: Heat induces sexual polyploidisation through 2n pollen

To investigate the impact heat induced meiotic defects on further pollen development, pollen size of Mt-0 was monitored for 10 days after a 24h at 32°C heat treatment using a Coulter Counter [33]. Pollen was collected from individual, freshly opened flowers along the main inflorescence on the morning of every new day (Supp. Figure 6a) and compared to a control that was kept at 20°C.

Under control conditions Mt-0 pollen samples form a Gaussian particle size distribution of which 90% of the particles consistently measure between 16µm-23µm (Supp. Figure 6b, d). We consider this to be normal-sized pollen. Smaller fractions consist of small particles (10µm-16µm; about 7%) and large particles (23µm-30µm; about 3%) which we consider to be mainly a mixture of dust and plant debris. After a 24h at 32°C heat treatment pollen quality was decreased compared to the control as indicated by an increase of small particles across 2-9 dpt (Supp. Figure 6c). On 3-4 dpt Alexander staining revealed the occurrence of shrivelled anthers filled with dead pollen (58 out of 107 anthers; Supp. Figure 6j), suggesting for a somatic defect harming all pollen in an anther during late pollen development. Contrary on 7-9 dpt, anthers appear swollen and contain a mixture of healthy (purple) and shrivelled (green) pollen (Supp. Figure 6k). This suggests a defect at the meiocyte/microspore level, of which the timing aligns with microspores receiving the heat treatment around the meiotic stage. Also, on 8-9 dpt the fraction of large particles strongly increases to an average of about 20% across all flowers analysed (Supp. Figure 6c). These large particles form a Gaussian peak around 25µm that is clearly separated from the normal-sized pollen (Supp. Figure 6e). DAPI staining of these samples reveals the presence of enlarged pollen grains with 1 enlarged vegetative and 2 enlarged sperm nuclei compared to the control Supp. Figure 6f-i). On 10 dpt pollen size was normal (Supp. Figure 6c) and viability fully recovered (Supp. Figure 6l), denoting the transient character of the effects of short term heat treatment.

Particle size analysis was also used to investigate other high dyad producing accessions (Supp. Figures 7 and 8). Under control conditions (20°C) most accessions show a Gaussian particle size distribution with a single peak around 20µm (Supp. Figure 8), exceptions are Etna-2, Sorbo, and Nok-3. These accessions consistently show next to a large peak at 20µm, respectively a small peak of enlarged particles around 25µm, a small peak of smaller particles around 18µm and a broad range of smaller particle between 10µm-20µm. The latter group of

small particles are likely empty pollen hulls generated by a heavy thrips infection on the Nok-3 plants. The occurrence of enlarged pollen in Etna-2 can be explained by this accession's high stature phenotype bringing its flowerbuds close to the heat emitting halogen lamps used in our growth rooms. This likely invokes diploid pollen production through meiotic restitution, in accordance with this accession's high dyad phenotype after heat. High temperatures (24h at 32°C) induced enlarged particles (>23µm) in most of these accessions on 8-10dpt (Supp. Figure 7). Exceptions are Nok-3, for which particle distributions do not differ remarkably from control conditions on these days, and Etna-2 that shows a nearly complete loss of detectable particles between 7-10dpt. In addition to a peak at 25µm some accessions showed a shift to even larger pollen sizes (30µm), suggesting the presence of higher level ploidy pollen (2n-4n [33]). From 10-11dpt pollen particle size distributions were similar to the 20°C control in all accessions, in accordance with the temporal impact of heat stress on pollen development (Supp. Figure 7).

Following our observations on the level of male meiosis and the known relationship between pollen ploidy and size [33] we assumed that the enlarged pollen of around 25µm after heat treatment never completed the second meiotic division, but nevertheless continued through microspore development to form mature pollen with a diploid (2n) chromosome number. To test this hypothesis, we used heat treated flowers of Mt-0 of 7-9 dpt as both male and female parents in a reciprocal manual cross with Mt-0 kept at 20°C as well as allowed heat treated plants to self. Afterwards the resulting offspring's ploidy was checked using flow cytometry. When heat treated Mt-0 was allowed to self or used as the male parent we detected triploid (3n) offspring on 8-9 dpt, consistent with the appearance of enlarged pollen on those days (Supp. Table 6). No triploids were detected in a cross with heat treated Mt-0 as the female parent. Nine out of 27 allegedly triploid plants were confirmed to be triploid (and not aneuploid) by counting the number of chromosomes on mitotic chromosome spreads (Supp. Figure 6m, n), indicating the viable 2n pollen after heat treating Mt-0 likely results from a clean omission of the second meiotic division.

Supplementary Note 2: histological examination of Mt-0 meiosis after different temperature treatments

Under control conditions (20°C) Mt-0 produces microspores organized in a tetrahedral configuration (100%, n=500), and surrounded by callose walls (Supp. Figure 9a, d, e). However, after a short heat treatment of 24h at 32°C, tetrad-stage flower buds mainly yielded dyads (81.2%, n = 2801), a minor fraction of triads (1.4%) and otherwise tetrads (17.4%) (Supp. Figure 9b-e). These dyads appeared balanced (i.e. both microspores appear equal in size and thus likely contain the same number of chromosomes), indicative for problems in cell wall formation, cytokinesis, or an arrest of the first or second meiotic division. Furthermore, callose walls separating and surrounding the microspores in a dyad configuration appeared thin and fragile in aniline blue stainings (25/34 dyads) (Supp. Figure 9c, Supp. Table 7). Visual inspection of the dyad configurations produced by other high dyad producing accessions revealed subtle histological differences (Supp. Figure 10 and Supp. Tables 7, 8 and 9). These included differences in the thickness of the callose wall separating the microspores (thin vs sturdy), differences in the number of nuclei in each microspore (1 or 2) and differences in the size of both microspores (equal or not). Accessions TOM03 and Sorbo also showed signs of cytomixis (Supp. Figure 10).

Histological examination of spread meiotic chromosomes shows that Mt-0 follows the canonical progression through male meiosis at 20°C (Supp. Figure 11a-h). After a 24h treatment at 32°C Mt-0 prophase chromosomes shows partial synapsis at pachytene (57%; n=98) and the loss of obligate cross over formation at diakinesis and metaphase I (19% and 19% as n=43 and 67; Supp. Figure 11i-k, q). Interactions between non-homologous chromosomes were observed (35%, n=43; Supp. Figure 11r), which did not occur at the control temperature, and anaphase I bridges and lagging chromosomes were observed frequently (71%, n=21; Supp. Figure 11l, t). These observations are in line with the previously described defects of Arabidopsis male meiosis at high temperatures[8]. Although chromosomes usually aligned on 2 perpendicular metaphase II plates (n=19; Supp. Figure 11n, v), the separation of the chromatids during anaphase II was never observed in any of the plants (n=9) analysed at high temperatures (Supp. Figure 11o, w), and meiosis concluded with the formation of dyads (57%, n=88), triads (16%) and tetrads (27%; Supp. Figure 11p, x). Altogether, these observations suggest that heat stress causes an arrest of metaphase II progression in Mt-0.

To further test the sensitivity of male meiosis in Mt-0 to temperature, flowering plants were subjected to 28°C and 32°C for different durations (Supp. Figure 9d). After 48h at 28°C, Mt-0 produced 1.8% dyads (n=764), a minor fraction of triads and otherwise normal tetrads (Supp. Figure 9e), indicating that male meiosis in Mt-0 is quite robust. Considering that male meiosis in Col-0 takes 26 hours from leptotene to the tetrad stage [63], a 24h heat treatment followed by immediate visualisation should reveal defects that originate from any of the meiotic substages (Supp. Figure 9d). The exposure of Mt-0 to 32°C for 12h resulted in 100% normal tetrads (n=538; Supp. Figure 9e) when analysed immediately after the treatment, indicating that high temperature did not affect cytokinesis or cell wall formation directly, but that dyad formation was likely the result of defects taking place during or right after meiosis I. Assuming that the duration of Mt-0 male meiosis is similar to that of Col-0, and that meiotic progression is generally accelerated at elevated temperature [39], heat treated plants were allowed to recover for 6 and 12 hours before tetrad microspore analysis. A 6h recovery at 20°C after heat caused an increase in the frequency of dyads and triads to 59.4% and 2.1% respectively (n=848), and after another 6h of recovery (for a total of 12h) the frequency of dyads and triads dropped again to 9.9% and 0.7% respectively (n=288) (Supp. Figure 9e). Taken together, these results show that dyad formation in Mt-0 is not a direct consequence of increased temperature during meiosis II, but rather originates from a defect during earlier meiotic stages from zygotene to the onset of meiosis II.

Cold stress is also known to induce meiotic restitution in Arabidopsis [64]. In order to find a link with the high temperature induced dyad phenotype, accessions Mt-0, Copac-1 and Vimmerby were subjected to 4°C for 48h. Sampling on time points 0h, 24h and 48h after the treatment revealed no excessive defects at the tetrad-stage (Supp. Figure 12), indicating that the molecular mechanisms that causes these accessions to be heat sensitive at the tetrad-stage does not confer a hypersensitivity to cold.

887

REFERENCES

1. Jiao, Y. *et al.* Ancestral polyploidy in seed plants and angiosperms. *Nature* **473**, 97–100 (2011).

2. De Storme, N. & Geelen, D. Sexual polyploidization in plants - cytological mechanisms and molecular regulation. *New Phytologist* **198**, 670–684 (2013).

3. Bretagnolle, F. & Thompson, J. D. Gametes with the somatic chromosome number: mechanisms of their formation and role in the evolution of autopolyploid plants. *New Phytologist* **129**, 1–22 (1995).

4. Kreiner, J. M., Kron, P. & Husband, B. C. Frequency and maintenance of unreduced gametes in natural plant populations: associations with reproductive mode, life history and genome size. *New Phytologist* **214**, 879–889 (2017).

5. De Storme, N. & Geelen, D. The impact of environmental stress on male reproductive development in plants: Biological processes and molecular mechanisms. *Plant Cell Environ* **37**, 1–18 (2014).

6. De Storme, N. & Geelen, D. Cytokinesis in plant male meiosis. *Plant Signal Behav* **8**, (2013).

7. Brownfield, L. & Köhler, C. Unreduced gamete formation in plants: Mechanisms and prospects. *J Exp Bot* **62**, 1659–1668 (2011).

8. De Storme, N. & Geelen, D. High temperatures alter cross-over distribution and induce male meiotic restitution in Arabidopsis thaliana. *Commun Biol* **3**, 1–15 (2020).

9. Magnard, J., Yang, M., Chen, Y. S., Leary, M. & Mccormick, S. Required for the Normal Pace and Synchrony of Cell Division during Male Meiosis 1. *Society* **127**, 1157–1166 (2001).

10. Wang, Y., Magnard, J. L., McCormick, S. & Yang, M. Progression through meiosis I and meiosis II in arabidopsis anthers is regulated by an A-type cyclin predominately expressed in prophase I. *Plant Physiol* **136**, 4127–4135 (2004).

11. d'Erfurth, I. *et al.* Turning meiosis into mitosis. *PLoS Biol* **7**, (2009).

12. Sofroni, K. *et al.* CDKD-dependent activation of CDKA;1 controls microtubule dynamics and cytokinesis during meiosis. *Journal of Cell Biology* **219**, (2020).

13. Zhu, J. *et al.* Slowing development restores the fertility of thermo-sensitive male-sterile plant lines. *Nat Plants* **6**, 360–367 (2020).

14. d'Erfurth, I. *et al.* The CYCLIN-A CYCA1;2/TAM is required for the meiosis I to meiosis II transition and cooperates with OSD1 for the prophase to first meiotic division transition. *PLoS Genet* **6**, 1–12 (2010).

15. Cromer, L. *et al.* OSD1 promotes meiotic progression via APC/C inhibition and forms a regulatory network with TDM and CYCA1;2/TAM. *PLoS Genet* **8**, (2012).

16. Bulankova, P., Riehs-Kearnan, N., Nowack, M. K., Schnittger, A. & Riha, K. Meiotic progression in Arabidopsis is governed by complex regulatory interactions between SMG7, TDM1, and the meiosis I-specific cyclin TAM. *Plant Cell* **22**, 3791–3803 (2010).

17. Cairo, A. *et al.* Meiotic exit in Arabidopsis is driven by P-body-mediated inhibition of translation. *Science (1979)* (2022).

18. Cifuentes, M. *et al.* TDM1 Regulation Determines the Number of Meiotic Divisions. *PLoS Genet* **12**, 1–22 (2016).

19. De Storme, N. & Geelen, D. The arabidopsis mutant jason produces unreduced first division restitution male gametes through a parallel/ fused spindle mechanism in meiosis II. *Plant Physiol* **155**, 1403–1415 (2011).

20. d'Erfurth, I. *et al.* Mutations in AtPS1 (Arabidopsis thaliana Parallel Spindle 1) lead to the production of diploid pollen grains. *PLoS Genet* **4**, 1–9 (2008).

21. Li, Y. *et al.* The type II Arabidopsis formin14 interacts with microtubules and microfilaments to regulate cell division. *Plant Cell* **22**, 2710–2726 (2010).

22. Brownfield, L. *et al.* Organelles maintain spindle position in plant meiosis. *Nat Commun* **6**, (2015).

23. Andreuzza, S., Nishal, B., Singh, A. & Siddiqi, I. The Chromatin Protein DUET/MMD1 Controls Expression of the Meiotic Gene TDM1 during Male Meiosis in Arabidopsis. *PLoS Genet* **11**, 1–22 (2015).

24. Wang, J., Li, D., Shang, F. & Kang, X. High temperature-induced production of unreduced pollen and its cytological effects in Populus. *Sci Rep* **7**, 1–12 (2017).

25. Pécrix, Y. *et al.* Polyploidization mechanisms: Temperature environment can induce diploid gamete formation in Rosa sp. *J Exp Bot* **62**, 3587–3597 (2011).

26. Schindfessel, C., Drozdowska, Z., De Mooij, L. & Geelen, D. Loss of obligate crossovers, defective cytokinesis and male sterility in barley caused by short-term heat stress. *Plant Reprod* **34**, 243–253 (2021).

27. Omidi, M., Siahpoosh, M. R., Mamghani, R. & Modarresi, M. The influence of terminal heat stress on meiosis abnormalities in pollen mother cells of wheat. *Cytologia (Tokyo)* **79**, 49–58 (2014).

28. Schindfessel, C., De Storme, N., Trinh, H. K. & Geelen, D. Asynapsis and meiotic restitution in tomato male meiosis induced by heat stress. *Front Plant Sci* **14**, (2023).

29. Karger, D. N. *et al.* Climatologies at high resolution for the earth's land surface areas. *Sci Data* **4**, 1–20 (2017).

30. Bomblies, K., Higgins, J. D. & Yant, L. Meiosis evolves: Adaptation to external and internal environments. *New Phytologist* **208**, 306–323 (2015).

31. Van de Peer, Y., Ashman, T. L., Soltis, P. S. & Soltis, D. E. Polyploidy: an evolutionary and ecological force in stressful times. *Plant Cell* **33**, 11–26 (2021).

32. Fox, D. T., Soltis, D. E., Soltis, P. S., Ashman, T. L. & Van de Peer, Y. Polyploidy: A Biological Force From Cells to Ecosystems. *Trends Cell Biol* **30**, 688–694 (2020).

33. De Storme, N., Zamariola, L., Mau, M., Sharbel, T. F. & Geelen, D. Volume-based pollen size analysis: An advanced method to assess somatic and gametophytic ploidy in flowering plants. *Plant Reprod* **26**, 65–81 (2013).

34. Xu, R. Y. *et al.* The Arabidopsis anaphase-promoting complex/cyclosome subunit 8 is required for male meiosis. *New Phytologist* **224**, 229–241 (2019).

35. Ormancey, M. *et al*. Complementary peptides represent a credible alternative to agrochemicals by activating translation of targeted proteins. *Nat Commun* **14**, (2023).

36. Sabi, R. & Tuller, T. Novel insights into gene expression regulation during meiosis revealed by translation elongation dynamics. *NPJ Syst Biol Appl* **5**, (2019).

37. Brar, G. A. *et al. High-Resolution View of the Yeast Meiotic Program Revealed by Ribosome Profiling*. vol. 335 www.sciencemag.org (2012).

38. Susor, A. & Kubelka, M. Translational regulation in the mammalian oocyte. in *Results and Problems in Cell Differentiation* vol. 63 257–295 (Springer Verlag, 2017).

39. De Jaeger-Braet, J., Krause, L., Buchholz, A. & Schnittger, A. Heat stress reveals a specialized variant of the pachytene checkpoint in meiosis of Arabidopsis thaliana . *Plant Cell* **34**, 433–454 (2022).

40. Matsuura, H., Ishibashi, Y., Shinmyo, A., Kanaya, S. & Kato, K. Genome-wide analyses of early translational responses to elevated temperature and high salinity in arabidopsis thaliana. *Plant Cell Physiol* **51**, 448–462 (2010).

41. Chen, K. *et al*. Translational Regulation of Plant Response to High Temperature by a Dual-Function tRNAHis Guanylyltransferase in Rice. *Mol Plant* **12**, 1123–1142 (2019).

42. Zhang, L. *et al*. Mutations in eIF5b confer thermosensitive and pleiotropic phenotypes via translation defects in Arabidopsis thaliana. *Plant Cell* **29**, 1952–1969 (2017).

43. Merchante, C., Stepanova, A. N. & Alonso, J. M. Translation regulation in plants: an interesting past, an exciting present and a promising future. *Plant Journal* **90**, 628–653 (2017).

44. Merret, R. *et al*. Heat-induced ribosome pausing triggers mRNA co-translational decay in Arabidopsis thaliana. *Nucleic Acids Res* **43**, 4121–4132 (2015).

45. Yángüez, E., Castro-Sanz, A. B., Fernández-Bautista, N., Oliveros, J. C. & Castellano, M. M. Analysis of genome-wide changes in the translatome of Arabidopsis seedlings subjected to heat stress. *PLoS One* **8**, (2013).

46. Kosmacz, M. *et al.* Protein and metabolite composition of Arabidopsis stress granules. *New Phytologist* **222**, 1420–1433 (2019).

47. Takahashi, N. *et al.* A regulatory module controlling stress-induced cell cycle arrest in Arabidopsis. *Elife* (2019) doi:10.7554/eLife.43944.001.

48. Ning, Y. *et al.* Heat stress interferes with formation of double-strand breaks and homolog synapsis. *Plant Physiol* **185**, 1783–1797 (2021).

49. Lardon, R., Wijnker, E., Keurentjes, J. & Geelen, D. The genetic framework of shoot regeneration in Arabidopsis comprises master regulators and conditional fine-tuning factors. *Commun Biol* **3**, 1–13 (2020).

50. Johnson-Brousseau, S. A. & McCormick, S. A compendium of methods useful for characterizing Arabidopsis pollen mutants and gametophytically-expressed genes. *Plant Journal* **39**, 761–775 (2004).

51. Ross, K. J., Fransz, P. & Jones, G. H. A light microscopic atlas of meiosis in Arabidopsis thaliana. *Chromosome Research* **4**, 507–516 (1996).

52. Bolger, A. M., Lohse, M. & Usadel, B. Trimmomatic: A flexible trimmer for Illumina sequence data. *Bioinformatics* **30**, 2114–2120 (2014).

53. Xu, H. *et al.* FastUniq: A Fast De Novo Duplicates Removal Tool for Paired Short Reads. *PLoS One* **7**, 1–6 (2012).

54. Andrews, S. *et al.* FastQC: a quality control tool for high throughput sequence data. *FastQC: a quality control tool for high throughput sequence data* http://www.bioinformatics.babraham.ac.uk/projects/fastqc (2014).

55. Sun, H. & Schneeberger, K. SHOREmap v3.0: Fast and Accurate Identifi cation of Causal Mutations from Forward Genetic Screens. in *Plant Functional Genomics: Methods and Protocols: Second Edition* (eds. Alonso, J. M. & Stepanova, A. N.) vol. 1284 381–395 (Springer, 2015).

56. Alonso-Blanco, C. *et al.* 1,135 Genomes Reveal the Global Pattern of Polymorphism in Arabidopsis thaliana. *Cell* **166**, 481–491 (2016).

57. Taylor, S. C. *et al.* The Ultimate qPCR Experiment: Producing Publication Quality, Reproducible Data the First Time. *Trends Biotechnol* **37**, 761–774 (2019).

58. Ahmed, M. & Kim, D. R. pcr: An R package for quality assessment, analysis and testing of qPCR data. *PeerJ* **2018**, (2018).

59. Alexander, M. P. Differential staining of aborted and nonaborted pollen. *Stain Technol* **44**, 117–122 (1969).

60. Vergne, P., Delvallee, I. & Dumas, C. Rapid assessment of microspore and pollen development stage in wheat and maize usind DAPI and membrane permeabilization. *Stain Technol* **62**, 299–304 (1987).

61. Galbraith, D. W. *et al.* Rapid flow cytometric analysis of the cell cycle in intact plant tissues. *Science (1979)* **220**, 1049–1051 (1983).

62. Capitao, C. *et al.* A CENH3 mutation promotes meiotic exit and restores fertility in SMG7-deficient Arabidopsis. *PLoS Genet* **17**, 1–26 (2021).

63. Prusicki, M. A. *et al.* Live cell imaging of meiosis in arabidopsis thaliana. *Elife* **8**, 1–31 (2019).

64. De Storme, N., Copenhaver, G. P. & Geelen, D. Production of diploid male gametes in Arabidopsis by cold-induced Destabilization of postmeiotic radial microtubule arrays. *Plant Physiol* **160**, 1808–1826 (2012).